Analysis of Acyl Fluxes through Multiple Pathways of Triacylglycerol Synthesis in Developing Soybean Embryos[1][W][OA]

Philip D. Bates, Timothy P. Durrett, John B. Ohlrogge, and Mike Pollard*

Departments of Biochemistry and Molecular Biology (P.D.B.) and Plant Biology (T.P.D., J.B.O., M.P.), Michigan State University, East Lansing, Michigan 48824–1312

The reactions leading to triacylglycerol (TAG) synthesis in oilseeds have been well characterized. However, quantitative analyses of acyl group and glycerol backbone fluxes that comprise extraplastidic phospholipid and TAG synthesis, including acyl editing and phosphatidylcholine-diacylglycerol interconversion, are lacking. To investigate these fluxes, we rapidly labeled developing soybean (*Glycine max*) embryos with [^{14}C]acetate and [^{14}C]glycerol. Cultured intact embryos that mimic in planta growth were used. The initial kinetics of newly synthesized acyl chain and glycerol backbone incorporation into phosphatidylcholine (PC), 1,2-*sn*-diacylglycerol (DAG), and TAG were analyzed along with their initial labeled molecular species and positional distributions. Almost 60% of the newly synthesized fatty acids first enter glycerolipids through PC acyl editing, largely at the *sn*-2 position. This flux, mostly of oleate, was over three times the flux of nascent [^{14}C]fatty acids incorporated into the *sn*-1 and *sn*-2 positions of DAG through glycerol-3-phosphate acylation. Furthermore, the total flux for PC acyl editing, which includes both nascent and preexisting fatty acids, was estimated to be 1.5 to 5 times the flux of fatty acid synthesis. Thus, recycled acyl groups (16:0, 18:1, 18:2, and 18:3) in the acyl-coenzyme A pool provide most of the acyl chains for de novo glycerol-3-phosphate acylation. Our results also show kinetically distinct DAG pools. DAG used for TAG synthesis is mostly derived from PC, whereas de novo synthesized DAG is mostly used for PC synthesis. In addition, two kinetically distinct *sn*-3 acylations of DAG were observed, providing TAG molecular species enriched in saturated or polyunsaturated fatty acids.

In plants, essentially all acyl chains for membrane and storage lipid synthesis are produced in the plastid by acyl carrier protein-dependent de novo fatty acid synthesis (Ohlrogge et al., 1979; Ohlrogge and Browse, 1995; Schwender et al., 2006). However, in oilseeds, these acyl groups are used almost completely (>95%) by the extraplastid pathways of glycerolipid synthesis, collectively termed the eukaryotic pathway (Roughan and Slack, 1982; Ohlrogge and Browse, 1995). The plastid acyl carrier proteins are hydrolyzed, and the free fatty acid end products (usually 18:1 > 16:0 > 18:0) are transported across the plastid envelope (Pollard and Ohlrogge, 1999; Koo et al., 2004). Once activated to acyl-CoAs (Andrews and Keegstra, 1983; Block et al., 1983), these acyl groups are available for incorporation by the acyltransferases of the eukaryotic pathway. Acyl-CoAs, as provided directly from de novo fatty acid synthesis and from other sources, can be used for the sequential *sn*-1 and *sn*-2 acylations of glycerol-3-phosphate (G3P) to produce phosphatidic acid (PA). PA is then converted to 1,2-*sn*-diacylglycerol (DAG) by the action of PA phosphatase. DAG represents an important branch point between neutral and membrane lipid biosynthesis. DAG may be acylated to produce triacylglycerol (TAG) or converted to phosphatidylcholine (PC) by CDP-choline:1,2-diacyl-*sn*-glycerol cholinephosphotransferase (CPT), with an analogous reaction to form phosphatidylethanolamine (PE). Desaturation of 18:1 to 18:2 and then 18:3 on PC produces the abundant polyunsaturated molecular species of PC (Sperling et al., 1993; Sperling and Heinz, 1993; Harwood, 1996).

In both leaves (Bonaventure et al., 2004) and seeds (Slack et al., 1978), the flux of nascent fatty acids (FAs) into PC dominates over the synthesis of PE and other phospholipids of the eukaryotic pathway. Recently, we investigated the initial steps in eukaryotic membrane lipid synthesis in expanding pea (*Pisum sativum*) leaves through in vivo labeling of the acyl

[1] This work was supported by the U.S. Department of Energy (grant no. DE–FG02–87ER13729), by the Department of Energy Great Lakes Bioenergy Research Center (www.greatlakesbioenergy.org) supported through the U.S. Department of Energy Office of Science, Office of Biological and Environmental Research, Cooperative Agreement DE–FC02–07ER64494, and by the National Research Initiative of the U.S. Department of Agriculture Cooperative State Research, Education, and Extension Service (grant no. 2005–35504–16195).

* Corresponding author; e-mail pollard9@msu.edu.

The author responsible for distribution of materials integral to the findings presented in this article in accordance with the policy described in the Instructions for Authors (www.plantphysiol.org) is: Mike Pollard (pollard9@msu.edu).

[W] The online version of this article contains Web-only data.

[OA] Open Access articles can be viewed online without a subscription.

www.plantphysiol.org/cgi/doi/10.1104/pp.109.137737

groups and backbones of glycerolipids (Bates et al., 2007). The results were inconsistent with a pathway in which newly synthesized FAs are directly esterified to G3P during de novo glycerolipid synthesis. We use "de novo" to describe glycerolipid synthesis in which the metabolic steps under consideration include the incorporation of the glycerol backbone. Instead, almost all newly synthesized FAs were esterified to a *sn*-1 or *sn*-2 lyso-PC through an acyl editing process resulting in molecular species of PC with one newly synthesized and one previously synthesized FA. In contrast, de novo glycerolipid synthesis in pea leaves primarily used recycled acyl groups released from PC during acyl editing. Acyl editing, also termed "remodeling" or "retailoring," is defined as any process that exchanges acyl groups between polar lipids but that does not by itself result in the net synthesis of the polar lipids. Acyl editing may proceed by at least two mechanisms. The first mechanism involves CoA:PC acyl exchange producing lyso-PC and acyl-CoA. This pathway was demonstrated in microsomes isolated from developing seeds and was attributed to a reverse reaction of lysophosphatidylcholine acyltransferase (LPCAT; Stymne and Stobart, 1984). There are several reports of high LPCAT activity in seeds (Rochester and Bishop, 1984; Stymne and Stobart, 1984; Bafor et al., 1991; Demandre et al., 1994; Ichihara et al., 1995). A second possible mechanism for acyl editing involves hydrolysis of PC to lyso-PC by a phospholipase activity, activation of the released free FA, and its reuse for phospholipid synthesis from lyso-PC by LPCAT. This mechanism is sometimes called "the Lands' cycle" (Lands, 1965; Shindou and Shimizu, 2009).

Plants exhibit both acyltransferase and transacylase mechanisms for the acylation of DAG to TAG. Three classes of 1,2-*sn*-diacylglycerol:acyl-CoA acyltransferases (DGATs) have been identified in plants, namely, the endoplasmic reticulum (ER) membrane-bound DGAT1 (Hobbs et al., 1999; Zou et al., 1999) and DGAT2 (Lardizabal et al., 2001; Shockey et al., 2006) classes and a soluble cytosolic DGAT class (Saha et al., 2006). In the context of plant lipid biochemistry, the term "Kennedy pathway" is often used to describe the direct conversion of G3P to produce TAG by sequential *sn*-1, *sn*-2, and *sn*-3 acyl-CoA-dependent acylations (Stymne and Stobart, 1987; Napier, 2007). In addition, the transacylase phospholipid:diacylglycerol acyltransferase (PDAT) allows the transfer of acyl groups from the *sn*-2 position of PC to DAG, producing TAG and lyso-PC products (Dahlqvist et al., 2000). The lyso-PC product is presumably rapidly reacylated by LPCAT. A DAG:DAG transacylase activity that produces TAG and monoacylglycerol has also been described (Stobart et al., 1997).

In addition to this diversity of TAG synthesis mechanisms and biosynthetic genes, oil-accumulating tissues may use different strategies to enrich for polyunsaturated fatty acids (PUFAs) in TAG. PC is the major site of eukaryotic pathway FA desaturation (Sperling et al., 1993; Sperling and Heinz, 1993) and related reactions, whereas evidence for a direct role for DAG or TAG as a desaturase substrate is lacking. The conversion of PC to DAG (for TAG synthesis) may enrich for PUFAs in TAG. This conversion may be accomplished by the reverse action of CPT or by a phospholipase C (Slack et al., 1983, 1985). Secondly, PUFAs may be enriched in TAG by PC acyl editing mechanisms that increase the PUFA content of the acyl-CoA pool. A third enrichment mechanism arises from the direct transfer of acyl groups from PC to DAG by the action of PDAT in TAG synthesis.

It is clear that there are a number of alternative metabolic routes for TAG synthesis. The alternatives may vary with tissue, species, and development and include the recycling of intermediates of membrane lipid biosynthesis. Different metabolic labeling experiments have been used to probe the sequence of reactions for TAG synthesis in vivo from a variety of oilseed species. Use of a PC-derived DAG moiety has been proposed as the major pathway for TAG synthesis in excised linseed (*Linum usitatissimum*) and soybean (*Glycine max*) cotyledons (Slack et al., 1978). Glycerol backbone labeling of developing safflower (*Carthamus tinctorius*) cotyledons suggested that the DAG pool feeding TAG synthesis was in equilibrium with PC (Griffiths et al., 1988a). However, in the same study, a similar experiment with avocado (*Persea americana*) mesocarp suggested that PC was not involved in TAG synthesis. This led the authors to propose that PC backbone turnover is used primarily in high PUFA-containing TAG synthesis. Phosphocholine head-group labeling in linseed cotyledons was also consistent with the concept that DAG equilibrates with PC, allowing the production of a highly unsaturated DAG pool prior to incorporation into TAG (Slack et al., 1983). The authors suggested that the reversible CPT reaction is most likely responsible for this phosphatidylcholine-diacylglycerol interconversion. Labeling of safflower cotyledon slices with free FAs allowed an alternative mechanism for PUFA enrichment in TAG to be proposed. An *sn*-2-specific LPCAT could direct 18:1 toward desaturation on PC and release PUFA to the acyl-CoA pool for the Kennedy pathway (Griffiths et al., 1988b). Although there is now significant in vivo evidence for PC acyl editing in the eukaryotic pathway in plant leaves (Bates et al., 2007), much less in vivo evidence for such a cycle in oilseeds exists.

We took several steps to extend and improve on previous studies of oilseed metabolism to determine the pathway of FA and glycerol incorporation into membrane and storage lipids in soybeans. To avoid potential artifacts associated with wounding due to excision of tissues, we used cultured soybean embryos that closely mimic in planta growth and oil accumulation (Allen et al., 2009). To provide an analysis of the initial events in eukaryotic glycerolipid synthesis, we performed kinetic labeling studies with time points shorter than previous studies. Labeling was conducted with both [^{14}C]acetate and [^{14}C]glycerol, and the labeled compositions, regiospecificity, and molecular

species of labeled PC, DAG, and TAG, along with endogenous molecular species compositions were determined. Together, these approaches have allowed us to develop a more quantitative flux model of soybean glycerolipid synthesis in vivo that demonstrates that acyl editing of PC is a dominate flux in TAG synthesis.

RESULTS

Embryo Culture and Endogenous Lipid Compositions Mimic in Planta Growth

Relationships between precursor and product pools in metabolic pathways are revealed by kinetic labeling experiments. However, accurate interpretation of metabolic labeling studies requires that during labeling the tissue functions as it would in vivo. In this context, the use of cultured embryos (as opposed to embryo or seed slices in simple buffered media) minimizes lipase activation and other perturbations of lipid metabolism due to wounding. Therefore, we used a soybean embryo culture system that allows dissected zygotic embryos to closely mimic in planta embryo development for >2 weeks (Allen et al., 2009). Radioactive precursors are added at low concentrations ([^{14}C]acetate and [^{14}C]glycerol at 0.5–1 mM) relative to the culture media, which also contains Suc (140 mM), Glc (70 mM), and amino acids (48 mM) at levels that mimic the apoplastic concentration surrounding the embryo in planta. This minimizes changes in metabolism that might occur due to alternative carbon source use during the labeling.

Developing soybean embryos of 15 to 20 mg dry weight were precultured for 3 d before addition of radioactive substrates to allow metabolism to equilibrate past any transient response due to the initiation of embryo culture. Cultured embryos accumulate about 6 mg total biomass per day (Allen et al., 2009). Therefore, each embryo doubles in biomass during the preculture. In cultured soybean embryos, DAG and PC had very similar FA compositions (Table I) and molecular species profiles (Fig. 1A). FAs are desaturated on PC, but it is DAG that is the precursor for TAG. Thus, the combined PC/DAG pool is expected to provide precursor DAG for TAG synthesis. TAG FA composition and molecular species distribution are shown in Table I and Figure 1B, respectively. The TAG molecular species analysis is similar to that reported for 35 to 40 d after flowering field-grown soybeans (Roehm and Privett, 1970).

The linear accumulation of a product, once reached, coincides with steady state labeling of all precursor

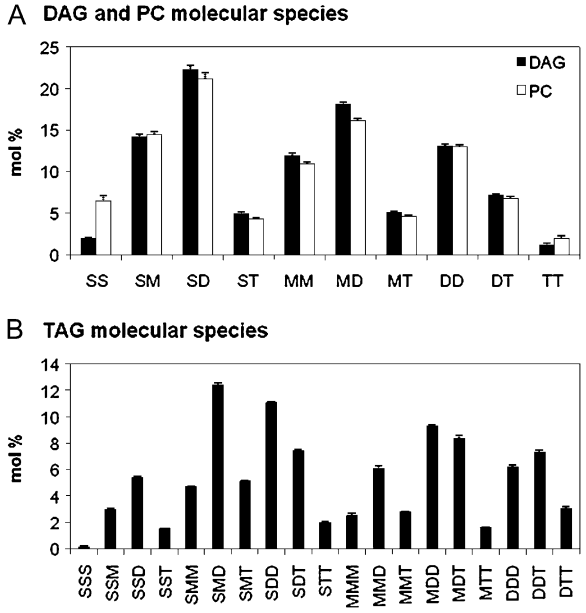

Figure 1. Endogenous molecular species compositions of DAG, PC, and TAG from developing soybean embryos of 13 to 14 mg dry weight per embryo precultured for 3 d, as determined by ESI-MS/MS. Molecular species are represented as two or three FAs (no stereochemistry specified). Bar heights represent mol % of each species among the total. For comparison to radiolabeled molecular species separated by argentation TLC as shown in later figures, the molecular species here are grouped based on the individual FA number of double bonds: total saturates (16:0, 18:0, 20:0, etc.), S; monoenes (18:1), M; dienes (18:2), D; and trienes (18:3), T. Full molecular species measurements of the nongrouped lipid molecular species for TAG, DAG, and PC are in Supplemental Tables S1 and S2, respectively. A, DAG (black bars) and PC (white bars). B, TAG.

Table I. *Endogenous lipid pool sizes and FA composition*

DAG, PC, and TAG amounts present in 13 to 14 mg dry weight developing embryos precultured for 3 d, as measured by ESI-MS/MS. The FA composition is calculated from the molecular species in Figure 1. FA values are represented as mol % among each lipid class.

	DAG	PC	TAG
nmoles lipid embryo^{-1}	104.1 ± 25.3	270.5 ± 27.8	4,658.8 ± 179.0
% mol FA			
16:0	14.4 ± 0.4	17.2 ± 0.4	14.9 ± 0.3
18:0	8.2 ± 0.4	9.4 ± 0.3	4.6 ± 0.05
18:1	30.6 ± 0.3	28.6 ± 0.2	26.4 ± 0.2
18:2	36.9 ± 0.3	35.0 ± 0.5	41.2 ± 0.2
18:3	9.9 ± 0.3	9.9 ± 0.3	12.3 ± 0.1
20:0			0.7 ± 0.05

pools. For this reason, the duration of labeling needs to be short enough so that precursor pools have not filled before time point sampling begins. Developing soybeans produce approximately 2.7 nmol FA min^{-1} $embryo^{-1}$ (Allen et al., 2009). As approximately 90% of newly synthesized FAs are used to produce TAG, of which one-third are used for *sn*-3 acylation, then the flux through the DAG precursor pool into TAG is approximately 1.6 to 2.7 nmol FA min^{-1} $embryo^{-1}$, depending on the origin of the *sn*-3 acyl group. Therefore, turnover time of the combined DAG/PC pool (750 nmol FA, based on Table I) would be 4.6 to 7.8 h if all the DAG and PC take part in acyl metabolism. Thus, our assays of 2 to 30 min will be effective measures of initial rates and products but will not directly measure the long-term precursor-product relationships of FA flux through DAG into TAG. However, as described below, longer term relationships can be inferred through full analysis of labeled lipid molecular species and consideration of the endogenous end point compositions.

[^{14}C]Acetate-Labeled FA Products

[^{14}C]Acetate is an ideal substrate for the study of acyl lipid metabolism because it rapidly enters plant tissue and is highly specific for incorporation into newly synthesized FA. After incubations of [^{14}C]acetate with cultured soybean embryos, transmethylation of total lipid extracts resulted in ≥96% of the radioactivity recovered in the hexane soluble fraction. Thin-layer chromatography (TLC) analysis of total lipids at 10 min of labeling indicated ≤9% of the radioactivity migrated with free sterols or waxes. Thus, >87% of [^{14}C]acetate incorporated into soybean lipids is in the acyl moiety of glycerolipids. The rate of [^{14}C]acetate incorporation into the soybean lipid acyl fraction was 2.2 nmol [^{14}C]acetate $embryo^{-1}$ min^{-1} (Fig. 2). This is approximately one-tenth of the rate of FA synthesis in embryos when expressed on a C2 unit incorporation basis (24 nmol acetyl-CoA $embryo^{-1}$ min^{-1}; Allen et al., 2009). Therefore, assuming an equal distribution and use of acetate within the embryo tissue, statistically, most of the FAs synthesized during the labeling period contained a single [^{14}C]C2 unit. [^{14}C]Oleate (18:1) and [^{14}C]saturated FA (16:0 and 18:0) are the immediate products of FA synthesis (Supplemental Fig. S1). Total labeled saturates increased from 23% of total FA at 2 min to 42% by 30 min of labeling. At 30 min of labeling, <3% of the labeled FA were desaturated to [^{14}C]linoleate (18:2); therefore, short time point labeling represents the initial acyl transferase reactions of newly synthesized FA, prior to further metabolism. Further details on the labeling of saturates are given online (Supplemental Figs. S1 and S2; Supplemental Methods for Supplemental Fig. S2).

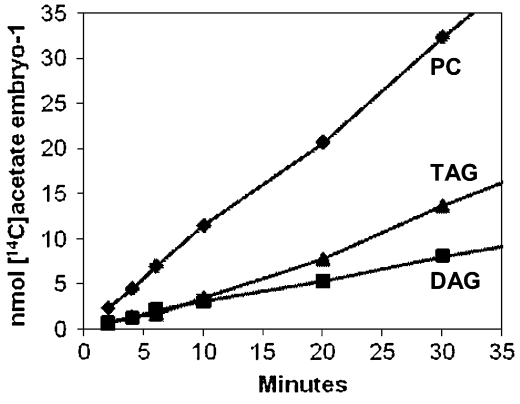

Figure 2. Time course for [^{14}C]acetate incorporation into the acyl groups of the major labeled soybean embryo lipids. Results expressed as nmoles of [^{14}C]acetate incorporated per embryo for each lipid. Data shown are from one representative labeling experiment. A second [^{14}C]acetate labeling experiment demonstrated similar kinetic relationships between PC, DAG, and TAG. Diamonds, PC; triangles, TAG; squares, DAG.

Kinetics of [^{14}C]Acetate Labeling Indicate Independent Acylations for Major Lipid Classes

To determine the initial rates and precursor-product relationships for the incorporation of newly synthesized FA into soybean glycerolipids, we followed [^{14}C]acetate labeling into the major labeled soybean embryo lipids (Fig. 2). At all time points, PC, DAG, and TAG represent approximately 85% of labeled glycerolipids. PC labeling was linear and gave the highest initial rate (1.15 nmol [^{14}C]acetate $embryo^{-1}$ min^{-1}, as determined from the first three time points). DAG labeling was also linear over the 30-min period and gave a lower initial rate (0.36 nmol [^{14}C]acetate $embryo^{-1}$ min^{-1}). The initial rate of TAG labeling was the lowest of the three major species (0.26 nmol [^{14}C]acetate $embryo^{-1}$ min^{-1}). However, TAG labeling accelerated and TAG accumulated more total radioactivity than DAG over time. Other membrane lipids contained very little of the newly synthesized FA. PE contained <8% of the radioactivity observed in PC even though PE mass abundance is approximately half that of PC (data not shown). PA is an intermediate of de novo glycerolipid synthesis, but PA labeling was barely detectable (<2% of that for PC; data not shown). In a separate [^{14}C]acetate labeling experiment, PC, DAG, and TAG were labeled in similar proportions and accounted for approximately 85% of labeled glycerolipids. The kinetics was similar with linear labeling of PC and DAG and an accelerating accumulation of label into TAG (data not shown).

As shown in Figure 2, the rate of incorporation of nascent FA into PC is independent of the incorporation of nascent FA into DAG or TAG, indicating independent acylation reactions. The relative initial acylation rates for PC:DAG:TAG are approximately 10:3:2, respectively. Thus, initial incorporation of newly synthesized FAs into extra plastidic glycerolipids is 57% PC, 17% DAG, and 11% TAG. The high rate of newly synthesized FA incorporation into PC is similar to the acyl editing described for membrane lipid production

in pea leaves where PC is the first incorporation product of chloroplast exported nascent FA (Bates et al., 2007). The accelerating rate for TAG synthesis over the 30-min period most likely reflects the movement of labeled diacylglycerol moieties from DAG and PC pools to TAG becoming measurable, although longer term assays will be required to detect concomitant reductions in DAG and PC labeling. A lesser contribution to the accelerating TAG labeling rate may arise from an increasing incorporation of very-long-chain saturates (≥C18).

[^{14}C]Acetate-Labeled FA Compositions Differ among Glycerolipid Classes

Fatty acid methyl esters (FAMEs) of PC, DAG, and TAG were separated by argentation TLC to determine [^{14}C]FA composition based on the number of double bonds (Fig. 3). At 2 min of labeling, [^{14}C]oleate made up >95% of the labeled FA in PC, while in DAG and TAG, the oleate levels were 78% and 44%, respectively. Total labeled saturates in PC slowly increased from <5% to approximately 25% at 30 min (Fig. 3A). In contrast, total labeled saturates were relatively constant in DAG and TAG over the first 30 min of labeling (Fig. 3, B and C). The average amount of saturated FA labeling between 4 and 30 min is 29% in DAG and 75% in TAG. The lower amount of labeled saturates at 2 min was most likely due to precursor acyl group pool filling. By 120 min, radioactivity is detected in PUFAs in all lipids, and the relative proportions of saturates have dropped as the newly synthesized FAs are slowly equilibrated through metabolism to more closely reflect the endogenous FA compositions. The very different initial [^{14}C]FA compositions among PC, DAG, and TAG (Fig. 3) reflect different metabolic processes for incorporation of nascent FA into glycerolipids. These are consistent with their independent acyl labeling kinetics (Fig. 2).

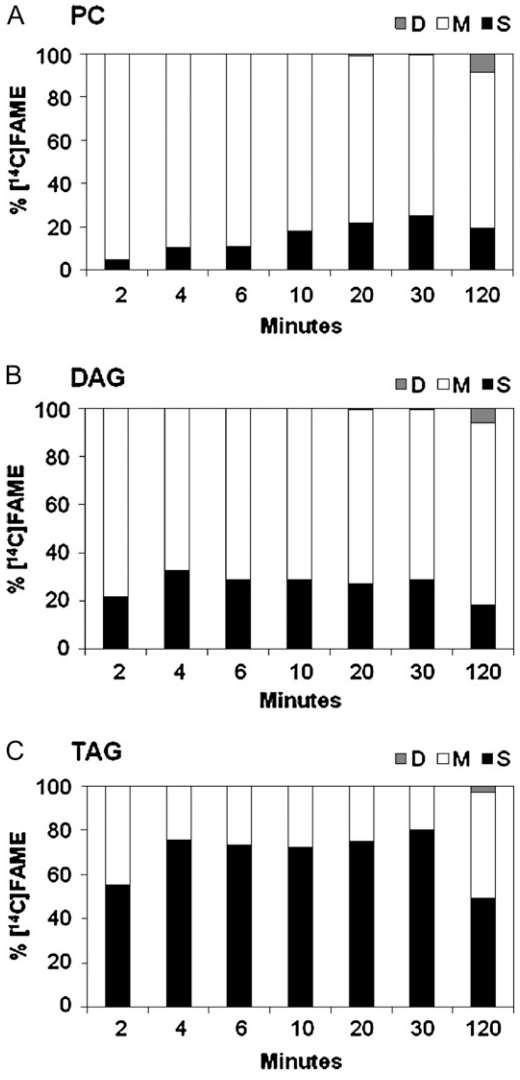

Figure 3. Radiolabeled FA composition of [^{14}C]acetate-labeled lipids presented in Figure 2. Each bar shows the distribution of radioactivity among different acyl groups at each time point. Bar shading: total saturates, S, black; monoenes (18:1), M, white; and dienes (18:2), D, gray. A, PC; B, DAG; C, TAG.

Positional Distributions of [^{14}C]Acetate-Labeled FA Differ among Glycerolipid Classes

The regiospecificity of labeled FA distributions in PC, DAG, and TAG was determined by lipase or phospholipase digestion (Fig. 4). At 2 min, 86% of the newly synthesized FA in PC was esterified at the *sn*-2 position (Fig. 4A). An increase in *sn*-1 labeling from 14% to 26% by 10 min was largely a consequence of increased saturates. The unequal distribution of nascent FA incorporation into PC is reminiscent of our previous results in pea leaves at 5 min, in which acyl editing produced PC labeling at *sn*-1 and *sn*-2 positions of 38% and 62%, respectively (Bates et al., 2007). However, acyl editing in soybean embryos appears to be more active at the *sn*-2 position than in pea leaves. The increase in PC *sn*-1 saturate labeling may reflect a slow conversion of de novo-synthesized DAG into PC.

The regiospecificity of newly synthesized [^{14}C]FA acylation in DAG differed substantially from that of PC, in that at 2 min of labeling there was more *sn*-1-labeled FA (55%) than *sn*-2-labeled FA (45%; Fig. 4B). The relative *sn*-1 to *sn*-2 positional labeling equilibrated in DAG by 20 min. A possible cause for this equilibration is that a slow conversion of highly *sn*-2 labeled PC to DAG balances out the higher *sn*-1 labeling bias for the de novo-synthesized DAG. Since PC labeling at 20 min is >4 times that of DAG (Fig. 2), the proportion of labeled PC moving back to DAG must be minor, otherwise the DAG regiospecificity would reflect PC regiospecificity.

The results of the positional analysis of nascent [^{14}C]FA incorporation into TAG differ from that of both PC and DAG. Lipase digestion of TAG indicates that almost the entire label at early time points was *sn*-1

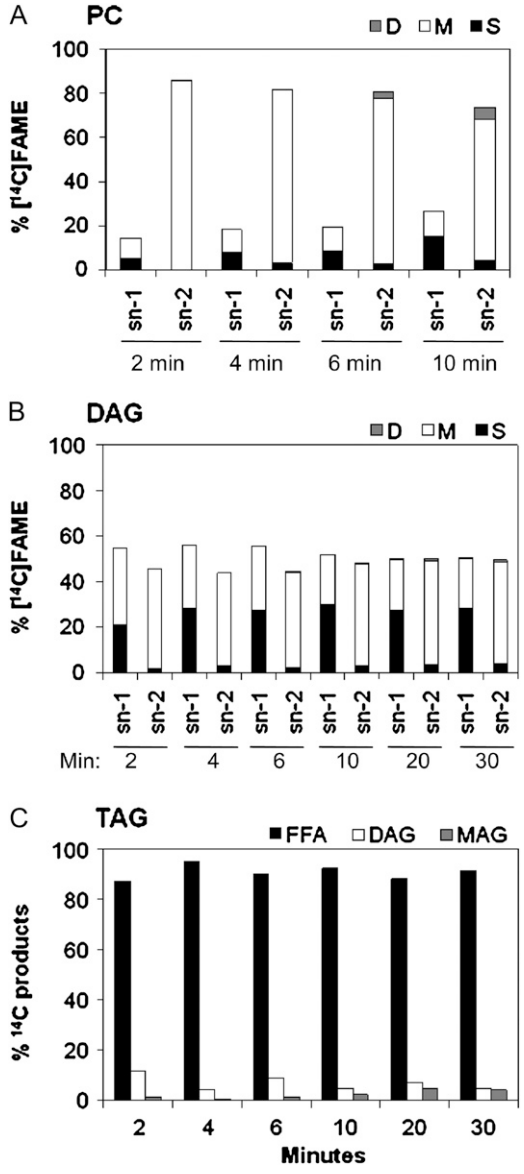

Figure 4. Positional analysis of [^{14}C]acetate-labeled acyl groups in different lipids. Major labeled lipids from the [^{14}C]acetate labeling time course were subject to lipase positional analysis. Bar heights represent percentage of lipid label in that position. A and B, Bar shading represents the labeled FA as a percentage of the whole lipid: total saturates, S, black; monoenes, M, (18:1), white; and dienes, D, (18:2), gray. A, PC. B, DAG. C, TAG. Bar shading: FFA (*sn*-1 or *sn*-3), black; DAG (*sn*-1,2 DAG or *sn*-2,3 DAG), white; MAG (*sn*-2), gray.

or *sn*-3 (Fig. 4C). Labeled FA can be incorporated into only the *sn*-3 position of TAG by acylation of an unlabeled DAG. Any *sn*-1 labeling must come from de novo synthesis of DAG. Since the DAG regiospecificity is approximately equal for *sn*-1 and *sn*-2 positions, the amount of label at *sn*-1 of TAG is predicted to be at most equal to the amount of label at *sn*-2. However, the end product of the lipase digestion, 2-*sn*-monoacylglycerol, is <2% of the total labeled end products (Fig. 4C). If any of the highly *sn*-2 labeled PC has been converted to DAG and then TAG, this would further reduce the relative amount of *sn*-1-labeled TAG compared with *sn*-2-labeled TAG. Therefore, we conclude that initial incorporation of nascent FA into TAG is almost completely localized to the *sn*-3 position.

Most [^{14}C]Acetate-Labeled PC and DAG Molecules Contain One Newly Synthesized FA

Molecular species analysis of intact labeled lipids can reveal information about unlabeled acyl group fluxes in biosynthetic processes. The unequal [^{14}C]FA positional labeling of DAG and PC suggest at least some nascent, labeled FA are incorporated into DAG and PC next to an unlabeled FA. To further investigate this facet of product structure, the molecular species of [^{14}C]acetate-labeled PC and DAG were separated and the labeled and unlabeled FA in each molecular species were determined (Fig. 5). At 2 min, the labeled molecular species SM made up 37% of total radioactivity in PC, with 36% as [^{14}C]M and only 1% as [^{14}C]S (Fig. 5A). Thus, 35% of the total PC must be [^{12}C]S[^{14}C]M, while only up to 2% of total PC could be the dual labeled species [^{14}C]S[^{14}C]M. The majority of other PC species (40%) consisted of unlabeled PUFA alongside a nascent labeled S or M (Fig. 5A). Assigning the labeled MM molecular species of PC (22%) precisely as single or dual acyl labeled is more problematic. Given that labeled oleate was highly incorporated at the *sn*-2 position in total PC, the possibility that MM was largely the dual labeled species is highly unlikely. Furthermore, at least 76% of nascent FAs were incorporated into PC alongside unlabeled S, D, or T in proportions relative to their endogenous composition and the position of acylation (Fig. 5A). Endogenous PC contained 30% M (Table I), which was almost as much as S and T together. Therefore, it is highly likely that nascent [^{14}C]S and [^{14}C]M were mostly incorporated next to endogenous unlabeled M in the labeled SM and MM molecular species, respectively.

The approximately equal distribution of [^{14}C]FAs between the *sn*-1 and *sn*-2 positions in DAG (Fig. 4B) could allow a very large proportion of labeled molecular species to contain two nascent FAs esterified to glycerol in one molecule. However, molecular species of [^{14}C]acetate-labeled DAG at 6 min (Fig. 5B) indicated that 56% of initial labeled molecular species contained a nascent labeled FA next to an unlabeled PUFA. In the labeled DAG molecular species SM, the unequal S and M labeling indicated that at least an additional 15% of total DAG is [^{12}C]S[^{14}C]M. Therefore, molecular species analysis of DAG indicates that at least 71% of DAG contains a newly synthesized FA incorporated in the same molecule as a previously synthesized FA. As with the PC, this analysis cannot reveal how much of the remaining SM and MM are singly or dually labeled, but it is probably much less than 29%. We conclude that initial [^{14}C]acetate-labeled PC and DAG are comprised predominantly of molecular

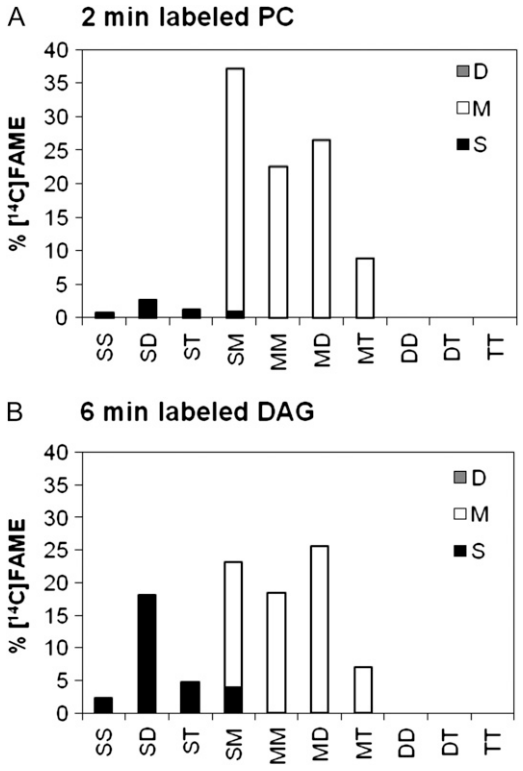

Figure 5. Molecular species compositions of [^{14}C]acetate-labeled PC and DAG. Molecular species were separated by argentation TLC. Nomenclature is as described in Figure 1. Bar height represents percentage of each species among total labeled species. Bar shading represents the amount of each radiolabeled FA in each species. Bar shading: S, total saturates, black bars; M, monoenes (18:1), white bars; and D, dienes (18:2), gray bars. Molecular species of labeled lipids were determined for the earliest time points that had enough radioactivity for the analysis. A, Two minute labeled PC; B, 6 min labeled DAG. Data for later time points are in given in Supplemental Figures S3 and S4.

species that contain one labeled (newly synthesized) FA and one unlabeled (previously synthesized) FA.

[^{14}C]Acetate-Labeled TAG Molecular Species Indicates Bulk DAG Was Used for *sn*-3 Acylation with Nascent [^{14}C]FA

At 6 min of [^{14}C]acetate labeling, the TAG molecular species distribution labeled with nascent FA is enriched in species containing S and M and is deficient in species containing two or three PUFA when compared to the endogenous molecular species distribution (Fig. 6A). The positional analysis described above indicated that nascent FA incorporation into TAG was primarily in the *sn*-3 position. Therefore, the [^{14}C]acetate-labeled TAG molecular species in Figure 6A each contain one labeled S or M and two unlabeled FA. The relative proportions of [^{14}C]S- and [^{14}C]M-labeled TAG are shown in Figure 6B. The calculated unlabeled [^{12}C]DAG molecular species composition for the precursor associated with the *sn*-3 [^{14}C]FA-labeled TAG was very similar to the endogenous bulk DAG and PC molecular species compositions (Fig. 6C). Therefore, it appears that DAG generated from the bulk PC pool is used for TAG synthesis with newly synthesized FA. Furthermore, inspection of Figure 6B reveals that there is little DAG selectivity when considering either [^{14}C]S or [^{14}C]M individually for esterification at the *sn*-3 position of DAG. However, this does not rule out selectivity of DAG molecular species for esterification of 18:2 or 18:3 to the *sn*-3 position.

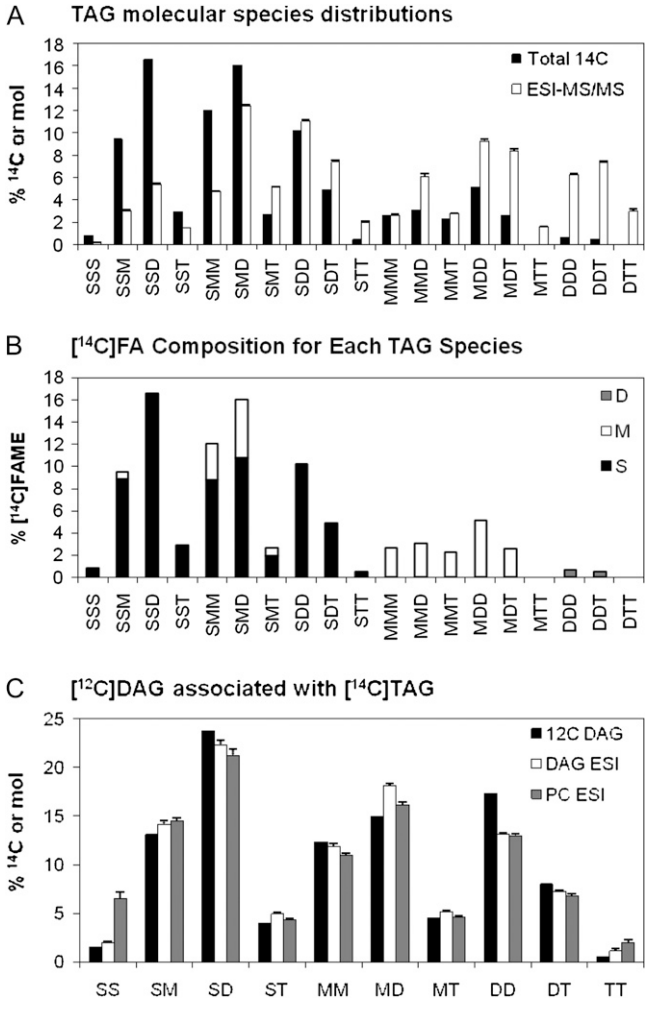

Figure 6. Analysis of TAG molecular species separated by argentation TLC after 6 min of labeling of soybean embryos with [^{14}C]acetate. Molecular species nomenclature as given in Figure 1. A, [^{14}C]Acetate-labeled molecular species (black bars) and endogenous molecular species from Figure 1 (white bars). B, Labeled FA composition within each molecular species of [^{14}C]acetate-labeled TAG. Bar shading represents the labeled FA within each molecular species: saturates, S, black; monoenes (18:1), M, white; dienes (18:2), D, gray; and trienes, T. C, Calculated unlabeled DAG molecular species associated with labeled TAG in B, assuming one *sn*-3-labeled FA per molecular species (black bars). Endogenous molecular species from Figure 1: DAG (white bars) and PC (gray bars).

Summary of [^{14}C]Acetate Labeling

The [^{14}C]acetate labeling kinetics, and the different labeled FA composition, positional acylation, and molecular species of DAG, PC, and TAG, reveal that newly synthesized DAG is not the precursor for nascent FA incorporation into either PC or TAG. Three different acyltransferase pathways are observed, namely, de novo glycerolipid synthesis via *sn*-1 and *sn*-2 acylations to produce DAG, PC acyl editing, and *sn*-3 acyl transfer to bulk DAG to produce TAG. These act independently of each other for the incorporation of nascent FA into glycerolipids. This clarifies ambiguities in previous seed labeling studies about the overlap of these pathways, at least for developing soybean embryos. The rapid labeling of PC mainly at the *sn*-2 position (Fig. 4A) suggests an acyl editing mechanism in which FAs are removed largely from the *sn*-2 position of PC to generate 1-*sn*-acyl-lyso-PC, which is then reesterified with newly synthesized FAs. By contrast, DAG is produced by the acyl-CoA-dependent G3P and lysophosphatidic acid acyltransferase reactions of de novo glycerolipid synthesis, which use nascent acyl groups mixed with unlabeled acyl groups to produce the approximately equal regiospecific labeling (Fig. 4B) and mixed molecular species labeling of [^{14}C]acetate-labeled DAG (Fig. 5B). Presumably most of the recycled unlabeled acyl groups used by de novo glycerolipid synthesis are released from PC during acyl editing. The labeled acyl composition (Fig. 3C), positional (Fig. 4C), and molecular species (Fig. 6) analyses of TAG at early time points demonstrate clearly that nascent FA are esterified to the *sn*-3 position of DAG by an acyltransferase system that is selective toward nascent saturates but not toward DAG molecular species. Furthermore, the DAG is likely derived from the bulk PC pool and not de novo-synthesized DAG. Direct incorporation of nascent FA by PC acyl editing, de novo DAG synthesis, and TAG synthesis from preformed DAG together account for approximately 85% of all newly synthesized FA incorporated into cytosolic glycerolipids, while the ratio of initial rates of incorporation (approximately 10:3:2, respectively, from Fig. 2) demonstrates that the major flux is a rapid acyl editing mechanism with PC, similar to our previous results in pea leaves (Bates et al., 2007).

[^{14}C]Glycerol Labeling of Lipid Backbones and Acyl Chains Indicates a Common Backbone Pathway and Separate Acylation Pathways among Lipid Classes

Lipids produced by de novo glycerolipid synthesis can be tracked with [^{14}C]glycerol, which is rapidly taken up by plant tissues and incorporated into the backbone of glycerolipids through G3P acylation (Slack et al., 1977, 1978, 1983; Bates et al., 2007). The initial rate of glycerol labeling of lipid backbones by developing soybeans was approximately 0.03 nmol glycerol min^{-1} embryo^{-1}, which corresponds to approximately 3.3% of the endogenous rate of glycerol incorporation into glycerolipids (approximately 0.9 nmol glycerol min^{-1} embryo^{-1}; Allen et al., 2009). The kinetics of [^{14}C]glycerol backbone labeling of PC, DAG, and TAG (Fig. 7A) was distinctly different from acyl labeling of glycerolipids by [^{14}C]acetate (Fig. 2). However, the kinetics of glycerol labeling of soybean embryos was qualitatively similar to that for developing linseed cotyledons (Slack et al., 1978). Other membrane lipids contained very little glycerol label. For example, PE contained <5% of the radioactivity observed in PC even though PE mass abundance is approximately half that of PC (data not shown). At the earliest time points, [^{14}C]glycerol labeling of the DAG backbone was already linear and was approximately 4 times the initial rate for PC and >8 times that of TAG. However, PC [^{14}C]backbone labeling rapidly accelerated such that by 30 min, PC contained more label than DAG and by 120 min it was approaching the approximately 5:2 molar ratio of endogenous PC:DAG (data not shown).

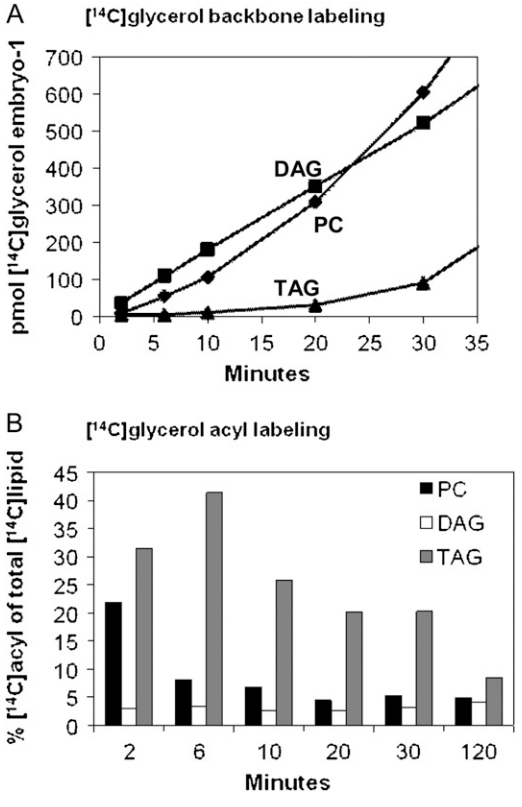

Figure 7. Time course for the incorporation of [^{14}C]glycerol into the backbone and acyl groups of the major labeled soybean embryo lipids. [^{14}C]Glycerol labeled lipids were transmethylated so that glycerol labeling and acyl labeling could be quantified separately. A, Kinetics of [^{14}C]glycerol backbone moiety labeling. Results expressed as pmoles [^{14}C]glycerol incorporated embryo^{-1}. B, Percentage of total lipid [^{14}C]glycerol labeling that is in the acyl chains over the time course. Bar shading: PC, black bars; DAG, white bars; and TAG, gray bars.

Thus, the DAG and PC labeling showed the expected precursor-product kinetic relationship of de novo glycerolipid synthesis. Incorporation of [^{14}C]glycerol into the backbone of TAG lagged significantly behind that of DAG and PC. TAG labeling was still accelerating after 120 min but had not reached the level of labeling observed for PC or DAG (data not shown) even though endogenous levels of TAG accumulate to approximately 20 times that of PC. The extreme lag of TAG (as compared to PC) behind DAG labeling suggests that the bulk of TAG synthesis (>98%) is not related to rapidly labeled de novo synthesis of DAG. TAG labeling is more consistent with a precursor-product relationship with PC. Therefore, the backbone labeling kinetics in developing soybeans are consistent with a major TAG synthesis pathway of G3P to DAG, to PC, to DAG, and finally to TAG. The results confirm and complement the molecular species analysis of [^{14}C]acetate-labeled TAG that revealed an unlabeled DAG moiety very similar to bulk DAG and PC (Fig. 6C).

In addition to backbone labeling, approximately 5% to 10% of label from [^{14}C]glycerol feeding is incorporated into acyl chains because G3P can also provide precursors for plastidic acetyl-CoA synthesis (Slack et al., 1977). The labeling of glycerol backbone and of acyl moieties were measured separately after lipid transmethylation. The labeled FA composition from [^{14}C]glycerol was very similar to that from [^{14}C]acetate (data not shown), indicating that de novo FA synthesis products were not dependent on the labeled substrate. Under steady-state conditions, [^{14}C]glycerol labeling of acyl and backbone precursor pools would result in a constant acyl to backbone labeling ratio. However, with rapid kinetic labeling, as shown in Figure 7B, the distribution of label from [^{14}C]glycerol between backbones and acyl groups varies with time for PC and TAG but not for DAG. At 2 min, PC contains 22% of the label in acyl chains, a value that drops to a steady-state level of approximately 5% by 20 min. This is consistent with rapid incorporation of nascent FA into PC through acyl editing while the backbone label lags through the de novo glycerolipid synthesis via the DAG pool. The constant approximately 5% acyl labeling of DAG over the time course represents nascent FA and backbone entering glycerolipids together by de novo G3P acylation. Initially, TAG contains the largest proportion of radiolabel in acyl chains, and it takes >120 min to approach the level of PC and DAG. This result also supports the hypothesis that nascent FA can be esterified at the *sn*-3 position to a DAG pool that is not immediately produced from de novo-synthesized DAG and that TAG steady-state labeling is consistent with backbone lagging through the large PC/DAG bulk pool. The dual acyl/backbone labeling from [^{14}C]glycerol confirms the conclusions made from separate [^{14}C]acetate acyl and [^{14}C]glycerol backbone labeling experiments of independent reactions for acyl group incorporation and a common de novo glycerolipid synthesis pathway for extraplastidic glycerolipids.

Analysis of Acyl Chains Used by de Novo Glycerolipid Synthesis

Separation of the [^{14}C]glycerol backbone-labeled lipid molecular species at early time points allows for analysis of the acyl groups used for acylation of G3P. The initial molecular species of backbone-labeled DAG and PC are very similar (Fig. 8, A and B, respectively), indicating that de novo-synthesized DAG is converted to PC without molecular species selectivity. The slightly higher SD and lower MM levels in labeled DAG compared to labeled PC might indicate a differential use of DAG molecular species by a low

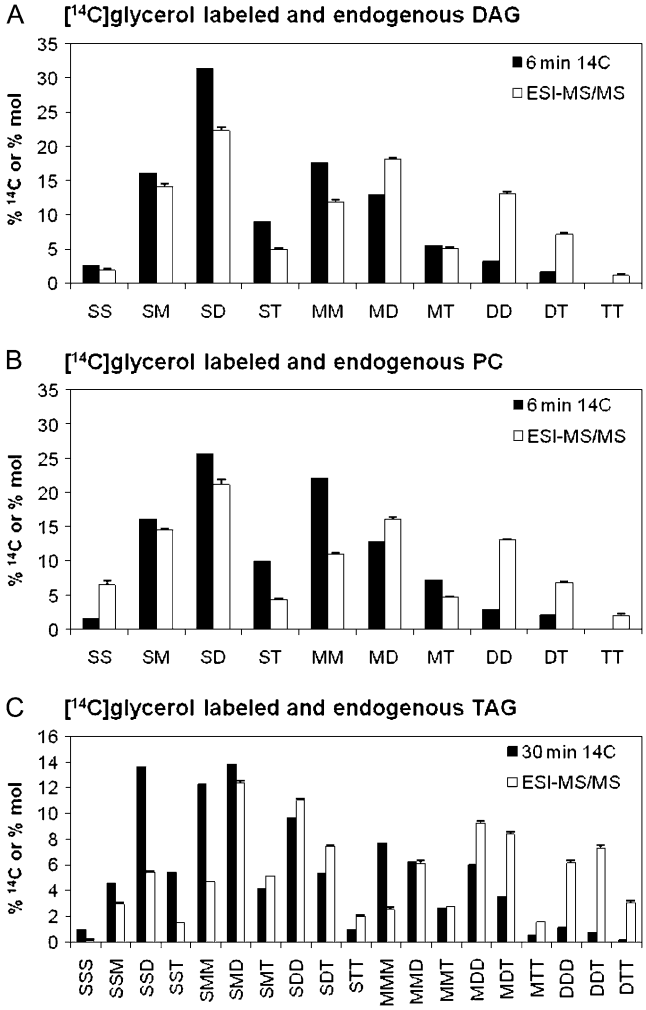

Figure 8. Molecular species composition of [^{14}C]glycerol backbone-labeled PC, DAG, and TAG. Molecular species are as defined in Figure 1. [^{14}C]Glycerol-labeled molecular species represent backbone labeling only (acyl chain labeling has been subtracted; black bars). Molecular species were determined at the earliest time point with enough radioactivity for analysis. The endogenous molecular species compositions are from Figure 1 (white bars). A, Six minute labeled DAG; B, 6 min labeled PC; C, 30 min labeled TAG. Additional 10- and 30-min time points for molecular species of DAG and PC are shown in Supplemental Figure S6.

flux pathway, such as for PE or phosphatidylinositol (PI) synthesis. The newly synthesized backbone labeled molecular species composition of PC and DAG contain relatively less polyunsaturated molecular species than the endogenous PC and DAG molecular species, respectively (Fig. 8, A and B; Supplemental Fig. S7). Our data are consistent with PC and DAG specific activity data reported for glycerol labeling of developing linseed cotyledons (Slack et al., 1983). Because acyl group desaturation is believed to occur on PC, but not DAG, de novo DAG has to be converted to PC for further desaturation. From this deduction and the observation that the bulk DAG pool molecular species profile (Fig. 1A) is similar to that used for TAG synthesis (Fig. 6B) and not to the de novo-synthesized DAG composition (Fig. 8A), we conclude that the immediately de novo-synthesized DAG can contribute only a relatively small fraction to the total endogenous DAG pool. Instead, the bulk of the endogenous DAG must be generated by another route. Since endogenous PC and DAG have very similar molecular species profiles (Fig. 1A), the bulk endogenous DAG production may involve the removal of the phosphocholine head-group from bulk PC to produce DAG by one of several possible mechanisms, such as a reversal of the CPT reaction or by phospholipase C action.

[^{14}C]Glycerol labeling of the TAG backbone was insufficient for molecular species analysis until 30 min of labeling. However, at 30 min, the [^{14}C]glycerol backbone-labeled TAG molecular species (Fig. 8C) showed a correspondence to that of initial [^{14}C]glycerol-labeled PC and DAG in that the labeled molecular species composition was relatively less polyunsaturated compared with the endogenous composition of the corresponding lipid. The calculated FA composition esterified to newly synthesized backbone labeled DAG, PC, and TAG was also very similar (Supplemental Fig. S7). Further interpretation of these results is presented below.

DISCUSSION

The goal of this study was to provide a quantitative analysis of acyl fluxes in the developing embryo of an oilseed, from the point where free FAs are exported from the plastid to the formation of TAG. The literature describing in vivo labeling of developing seeds suggests various metabolic pathways (for review, see Stymne and Stobart, 1987; Browse and Somerville, 1991; Napier, 2007). However, collectively, the studies suffer from a number of limitations: (1) The tissue is excised and immediately incubated, often in the absence of an osmoticum or nutrients. Thus, its physiological state relative to the in planta situation is uncertain. (2) It has been particularly difficult to assess flux directions and pools for the DAG-PC conversions. (3) Interpretation based on initial rates of reaction is underused, and there is often a lack of comprehensive product analysis. (4) Quantitative conclusions have rarely been possible. To undertake initial rate studies, we used both C2 and C3 precursors that discriminate between alternative pathways. These are rapidly taken up and used, with lag times $\leq$1 min, allowing the system to quickly reach a (quasi) steady-state labeling condition and hence allowing the opportunity to obtain initial rate data. By contrast, labeled hexose substrates will face very large dilutions; thus, the time required to reach a steady-state labeling will tend to obscure the initial kinetics of glycerolipid synthesis.

Newly Synthesized FAs Are Incorporated into Cytosolic Glycerolipids through at Least Three Independent Acyltransferase Pathways

Through analysis of the kinetics of glycerolipid acyl labeling from acetate, and analysis of the FA composition, position of acylation, and molecular species of these products, we demonstrate that three different acyltransferase systems are responsible for incorporation of newly synthesized FA into cytosolic glycerolipids. (1) The major flux of nascent FAs is through acyl editing of PC. The highest rate of FA incorporation was into PC (Fig. 2). There was no detectable kinetic lag to the onset of steady-state labeling of PC, indicating that PC is the immediate product of an acyltransferase using nascent FA. Although DAG is the precursor for net PC synthesis, the labeled FA composition (Fig. 3) and regiospecificity (Fig. 4) of the immediately labeled PC also indicated its formation was not related to the initial labeling of DAG. Molecular species (Fig. 5) and FA positional analyses of PC demonstrated that at least 75% of newly synthesized FAs in PC are esterified in molecules containing a preexisting FA. Finally, [^{14}C]glycerol acyl and backbone labeling (Fig. 7) showed that initial labeled acyl groups and the glycerol backbone are incorporated into PC independently. Together, these results reveal that approximately 57% of newly synthesized FAs are directly esterified to the *sn*-1 or *sn*-2 position of PC through acyl-editing mechanisms. We ascribe the acyl editing to acylation of yso-PC rather than a glycerophosphorylcholine acyltransferase activity because the latter activity has not been described in developing oilseeds, whereas microsomal *sn*-2 LPCAT and acyl exchange activities are high (Rochester and Bishop, 1984; Stymne and Stobart, 1984; Bafor et al., 1991; Demandre et al., 1994; Ichihara et al., 1995). (2) Newly synthesized FA mix with recycled FA to acylate G3P for de novo glycerolipid synthesis. Approximately 17% of newly synthesized FAs in glycerolipids were incorporated into DAG, and these acyl chains were approximately equally distributed between the *sn*-1 and *sn*-2 positions (Fig. 4). At least 71% of labeled DAG molecular species contained both a newly synthesized and a preexisting FA in the same molecule (Fig. 5). In contrast with PC, [^{14}C]glycerol acyl/backbone labeling demonstrated that nascent acyl groups and backbone are incorporated into DAG simultaneously (Fig. 7). These results demonstrate that the G3P and lysophosphatidic acid

acyltransferase of the eukaryotic de novo glycerolipid synthesis pathway use a mixed pool of acyl-CoA containing newly synthesized and recycled FA. The recycled FAs most likely originate from PC acyl editing. (3) Newly synthesized FAs were used for *sn*-3 acylation of preexisting DAG to generate TAG. Approximately 11% of newly synthesized FAs were directly incorporated into the *sn*-3 position of TAG, with negligible labeling in the *sn*-1 and *sn*-2 positions (Fig. 4). Nascent FA incorporation into TAG was kinetically independent of de novo DAG synthesis (Figs. 2 and 7), while TAG molecular species analysis indicated that the DAG precursor used had the same molecular species composition as the endogenous bulk DAG, which is derived from PC (Fig. 6). Therefore, the direct incorporation of nascent FA into TAG used a preexisting DAG pool, not de novo-synthesized (nascent) DAG. In a following section, we use the relative rates of these three independent acyl transferase pathways to construct a more quantitative model of TAG synthesis in soybeans.

At Least Two Systems of DAG *sn*-3 Acylation Producing TAG Can Be Identified

As mentioned above, 11% of the total FA labeling is directly incorporated into the *sn*-3 position of TAG. Other nascent FA are incorporated into glycerol lipids through acyl editing of PC and de novo DAG synthesis, which constitute approximately 57% and 17% of the total FA labeling, respectively. The remaining 15% of acyl label unaccounted in the above three glycerolipid classes is present largely in minor phospholipid species. As TAG constitutes approximately 93% of the endogenous acyl lipid mass, eventually approximately 31% of the nascent FAs must end up in the *sn*-3 position of TAG. Thus, approximately 20% of the nascent FAs incorporated into glycerolipids other than TAG must eventually move through into the *sn*-3 position of TAG to add to the 11% that are immediately incorporated. This represents a second, distinctive flux of FA into the *sn*-3 position of TAG.

When compared to endogenous TAG, the molecular species analysis of TAG from [^{14}C]acetate labeling (Fig. 6A) also strongly suggests two pathways to TAG. We estimated that TAG labeled with nascent FA at the *sn*-3 position provides approximately 35% of total TAG synthesis and has a total FA composition of 39% S, 29% M, 25% D, and 7% T, with the unlabeled DAG coming from the endogenous DAG pool (Fig. 6C) and *sn*-3 FAs made up of 75% S and 25% M (Fig. 3C). Since the endogenous TAG composition is 20% S, 27% M, 41% D, and 12% T, a separate contribution to TAG synthesis is required to provide the remaining 65% of TAG. This separate TAG synthesis must produce TAG of the composition 10% S, 26% M, 49% D, and 15% T so that together the two TAG synthesis systems can provide the endogenous TAG composition. It is clear that this second TAG synthesis component is distinctly different, containing reduced saturates and much higher PUFA than the initial [^{14}C]acetate-labeled TAG. The DAG moiety presumably comes from the bulk unsaturated DAG/PC pool, with a selectivity for *sn*-3 acylation for PUFA (approximately 85% D plus T). In addition, the molecular species analysis of [^{14}C]glycerol-labeled TAG (Fig. 8C) is also consistent with two pathways to TAG. We can group these molecular species of TAG into three groups: (1) high specific activity species SSS, SSM, SSD, SST, SMM, and MMM (approximately 16% of TAG endogenous mass); (2) low specific activity species MTT, DDD, DDT, DTT, and possibly STT, MDD, and MDT (approximately 20% of endogenous TAG mass), and (3) the other species, of intermediate specific activity (approximately 64% of endogenous TAG mass). High specific activity molecular species are dominated by high levels of S and M, consistent with the rapid labeling by nascent FAs, while slowly labeled species have high levels of D and T. Time is required for further desaturation of the PC species derived from de novo-synthesized DAG to eventually produce DAG species with both positions occupied by PUFA. These can then be used by the TAG synthesis system that acylates the *sn*-3 position with PUFA to produce TAG molecular species with all three positions occupied by PUFA. A PUFA selective DGAT or PDAT may be involved in this system.

A DAG/DAG transacylase (Stobart et al., 1997) has been proposed for the synthesis of TAG. Unsaturated FA would be transferred from the *sn*-2 position of one DAG molecule to the *sn*-3 position of another, producing TAG and a 1-*sn*-acyl-MAG. Reacylation of MAG by MAGAT using the mixed pool of nascent and recycled acyl-CoA would bring about a significant enrichment of label in the *sn*-2 position of DAG. This is not observed in Figure 4. Therefore, this pathway is not a major route of TAG synthesis in developing soybean embryos.

Interconversion of DAG and PC and Supply of DAG for TAG Synthesis

The interconversion of DAG and PC is already a firmly established facet of oilseed metabolism. It is often postulated to result from a highly reversible CPT (Slack et al., 1983, 1985; Triki et al., 1999). It has also been suggested that the PC and DAG pools may be in equilibrium (Roughan and Slack, 1982; Griffiths et al., 1988a). In this section, we consider various kinetic models that can describe the DAG-PC interconversion. To do this, we simulate DAG and PC pool filling for acyl and glycerol backbone fluxes for various kinetic models of the pathway to TAG. The details of this analysis are described online (Supplemental Discussion S1; Supplemental Figs. S8 and S9).

If there is no opportunity for PC conversion back to DAG, then TAG and PC synthesis would compete for the de novo DAG pool (Fig. 9, model A). In this simplest of cases, to generate the desired ratio of end products, the TAG backbone must label up about 20×

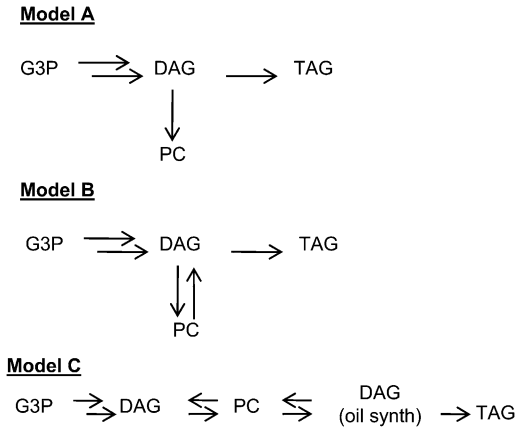

Figure 9. Representative flux models for TAG synthesis. A more extensive set of models that were tested by pool filling simulations of kinetic labeling experiments is shown in Supplemental Figure S9.

more rapidly than PC. However, the converse is observed: PC labels up about 10× more rapidly than TAG (Fig. 7A). Thus, any model for glycerolipid metabolism must include DAG-PC interconversion. We observed that the DAG pool used for *sn*-3 acylation with [^{14}C]acetate-labeled nascent acyl groups closely resembles the endogenous DAG and PC molecular species profiles (Fig. 6C) and not that of the de novo DAG pool (Fig. 8A). This is also consistent with DAG first moving to PC and then back to DAG. The simplest DAG-PC interconversion would be where both bulk PC and DAG are the biosynthetic pools (Fig. 9, model B). However, DAG-PC interconversion might result from more complex mechanisms, each of which may display distinctive kinetic consequences. Thus, for example, the DAG pool could be split into de novo (input) and oil synthesis (output) pools (Fig. 9, model C). A more comprehensive list of such mechanisms is supplied in Supplemental Figure S8. Pool filling simulations for models were run to see how closely they would conform to the experimental kinetics of glycerol backbone labeling shown in Figure 7A. Conditions were set to allow a simulation of glycerol backbone labeling from DAG that produced as close to continuous DAG labeling as possible but where PC labeling overtook DAG labeling at about 30 min, as in the experimental results (Fig. 7A). The backbone labeling models were then tested against the acyl chain labeling results (Fig. 2) to see how quickly acyl label would move from PC to DAG when PC was labeled through acyl editing. If the equilibration of [^{14}C]acetate-derived acyl label at the *sn*-1 and *sn*-2 positions of DAG is from PC conversion to DAG, in 30 min of assay no more than approximately 10% of the labeled acyl groups that accumulated in DAG can originate from PC (which is mostly *sn*-2-labeled through acyl editing; Fig. 4, A and B). However, the total acyl label in PC is 3 times that of DAG, so only approximately 3% of the total labeled acyl groups in PC originating from acyl editing can move through to DAG in 30 min. Simulations of acyl labeling using the simplest DAG-PC interconversion model, that is, for single PC and DAG pools (Griffiths et al., 1988b), failed to meet this criterion. By contrast, models that contained separate de novo and oil synthesis DAG pools (Fig. 9, model C; Supplemental Fig. S8, model C) were generally much more successful at describing the DAG-PC precursor-product glycerol labeling kinetics and yet have slow movement of acyl editing labeling of PC move through into DAG.

To further optimize the model and to allow for a more continuous DAG labeling and a greater acceleration of TAG labeling from glycerol, it was necessary to split the PC into two kinetically distinct pools and the DAG into three such pools. This iteration of the modeling is shown in Figure 10. More explicitly, the PC pool is split into a small, active pool and a large, bulk pool. If this is done, then acyl editing must be largely a function of the bulk pool and not the active pool; otherwise, the movement of acyl label from PC to DAG takes place too quickly. The DAG pool is split into a small de novo synthesis pool and a small pool that provides DAG for TAG synthesis and for DAG to

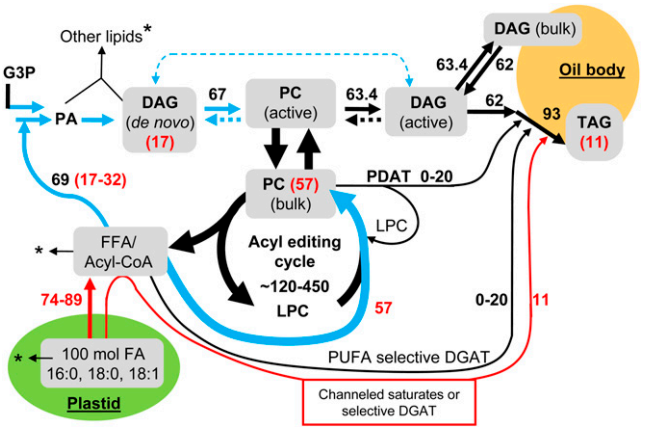

Figure 10. Soybean TAG synthesis acyl flux model. The assumptions and flux calculations are presented online. The model follows 100 mol of newly synthesized FA in the plastid through the major fluxes of lipid metabolism such that the final accumulations of FAs are TAG, 93 mol; PC, 3.6 mol; DAG, 1.4 mol; and other lipids, 2 mol. Other membrane lipids in soybean embryos are mostly PE and PI. The arrows indicate the fluxes, with the major metabolite pools proposed from kinetic analysis highlighted in gray. Dashed arrows represent uncertainty for that reaction. The black numbers represent total net steady-state fluxes or flux ranges as calculated online. The arrows highlighted in blue and red represent the major initial fluxes of newly synthesized FA as measured by [^{14}C]acetate labeling. Blue arrows represent fluxes where nascent and endogenous acyl groups mix, while red arrows indicate only nascent FA. The red numbers represent the initial accumulation of nascent FA into the major labeled glycerolipids PC, DAG, and TAG, which together accumulate approximately 85% of initial FA. Approximately 15% of nascent FA initially accumulates in lipids other than PC, DAG, and TAG. The asterisks represent small fluxes of acyl groups to these other lipids, for which products and/or mass flux analysis have not been determined.

move through into a bulk pool. This allows a small amount of labeled glycerol backbone to more rapidly traverse through PC to the DAG oil synthesis pool, and hence to TAG, while the majority of labeled glycerol backbone lags through the bulk PC and DAG pools prior to accumulating in TAG. In summary, the kinetics of [^{14}C]glycerol labeling suggest that the major flux of G3P through de novo synthesis into DAG is for PC synthesis, with almost none of the de novo-synthesized DAG being channeled directly to TAG. The conversion of de novo-synthesized DAG to PC is fairly rapid, but residence in the large PC pool is much longer to allow for further desaturation, before conversion back to DAG for TAG synthesis.

A Flux Model for Glycerolipid Synthesis in Developing Soybean Embryos

Our analysis of glycerolipid acyl group and glycerol backbone labeling enables us to generate a model of the flux of acyl groups during oil synthesis (Fig. 10). The individual elements of this model have already been discussed in the three preceding sections. A detailed step-by-step logic of model construction, along with its implicit assumptions and calculations, is presented online. The flux model structure is based on the kinetic model (Supplemental Fig. S9, model C, variant 3), which best fits the [^{14}C]acetate and [^{14}C]glycerol labeling data. The flux model tracks 100 mol of FAs synthesized in the plastid through lipid metabolism over a small time increment. The fluxes are determined based on initial rates of nascent FA incorporation into extraplastidic glycerolipids (Fig. 2), their composition, and molecular species (Figs. 3–6), along with determinations of the acyl groups used by de novo glycerolipid synthesis (Fig. 8). Endogenous lipid compositions (Table I, Fig. 1) and mass balance are also used to predict fluxes. Assuming steady-state metabolism, the end point reached in the developing soybean embryo accumulating oil will be 93 mol of acyl groups in TAG, 1.4 mol in DAG, 3.6 mol in PC, and 2 mol in other lipids (based on the values in Table I). The model shows the fluxes, or expected flux ranges, for both the newly synthesized FAs and for the total flux. It should be noted that in terms of an activity (expressed in moles FA accumulated unit time^{-1} unit fresh weight^{-1}), the relative rate of lipid synthesis in soybean is slow (approximately 5-fold less) compared to other oilseeds, such as safflower and rapeseed (*Brassica napus*). Thus, individual and relative acyl fluxes in other oilseeds may differ from that of soybean and will need to be determined independently.

Our simulations show a best fit when we describe lipid synthesis in terms of three kinetically distinct DAG pools and two PC pools. This is used as the basis for our model (Fig. 10). The DAG pool that is the immediate product of de novo glycerolipid synthesis and the DAG pool for TAG synthesis each contain only a small mole fraction of the total DAG, while the bulk DAG pool might be associated with the oil body fraction (Slack et al., 1980; Kuerschner et al., 2008). We cannot rule out the possibility that a very small fraction of the de novo DAG pool is used directly for TAG synthesis by the traditional Kennedy pathway, as indicated by the dotted arrow. Likewise, the reversibility of phosphatidylcholine-diacylglycerol interconversions is not clear: back reactions are indicated as dotted lines. An important aspect of PC metabolism is the acyl editing cycle, which represents the largest acyl flux in the cytosol and which is (mainly) associated with the bulk PC pool. We cannot place an exact value on this total flux (recycled plus nascent FA), but our analysis presented online suggests a lower limit of approximately 120 mol per time unit, which is twice the rate of nascent FA incorporation into PC and is almost twice the rate of total de novo glycerolipid synthesis. The upper limit is approximately 450 mol per time unit. In our study of acyl editing in pea seedlings (Bates et al., 2007), we considered the possibility that there was a channeled mole for mole exchange of nascent FAs with acyl groups released by acyl editing. However, if the acyl editing cycle flux is significantly larger than the incorporation of nascent acyl groups into PC via a PC:lyso-PC acyl editing cycle, then the simplest way to depict the process is via a bulk acyl-CoA pool where acyl groups released by acyl editing and from de novo FA synthesis mix, as shown in Figure 10.

Surprisingly, our labeling results suggested two kinetically distinct TAG synthesis systems. TAG synthesis will require 31 mol of acylation at the *sn*-3 position. Approximately 11 mol are provided by the immediate incorporation of nascent FA, with a high preference for saturates. Simulations and analysis of the molecular species of [^{14}C]FA-labeled TAG suggests that this direct acylation uses the DAG pool that is the output from PC, not the de novo-synthesized DAG pool produced by the Kennedy pathway. The high *sn*-3 [^{14}C]saturated FA labeling of bulk DAG suggest that either a specific pool of acyl-CoAs high in nascent saturates is delivered to a DGAT enzyme or that the DGAT has a strong selectivity for saturates from the bulk acyl group pool (Fig. 10). Because the explanation of TAG composition via two biosynthetic components, as discussed earlier, requires only the nascent saturates pool, without dilution by saturates from the acyl editing cycle, the former mechanism seems much more plausible.

Turning to the remaining 20 mol of FA, which are required for *sn*-3 acylation to produce TAG, at least two mechanisms, both of which are shown in Figure 10, may provide for this TAG synthesis, including essentially all the tri-PUFA TAG molecular species. A PUFA selective DGAT may use the bulk acyl pool or alternatively a PDAT reaction may transfer *sn*-2 PUFA from PC to DAG, generating TAG. The lyso-PC produced by a PDAT reaction will add an incremental flux to the PC acyl editing cycle (Fig. 10). It is noteworthy that the stereochemical analysis of TAG from soybean oil shows that the *sn*-1 and *sn*-3 positions have quite

similar acyl compositions (Brockerhoff and Yurkowski, 1966). Such observations have lead to speculations that the enzymes responsible for TAG synthesis are quite nonspecific. However, at least in soybean, there is the coincidental summation of two routes with distinct specificities to give the overall composition. PC has long been considered the site of FA desaturation. In developing soybeans acyl editing, the DAG → PC → DAG net conversion and a specific TAG synthesis system all contribute to the biosynthesis of TAG containing PUFA at higher levels than found in PC.

Linking the Model to Questions of Biochemistry and Cell Biology

Possible Biological Roles for Acyl Editing

Experiments demonstrating acyl exchange between acyl-CoA and the *sn*-2 position of PC in microsomes from many oilseeds, and the evidence that this was catalyzed through reversibility of LPCAT, are reviewed by Stymne and Stobart (1987). Acyl exchange was suggested as a mechanism to allow enrichment of PUFA for TAG synthesis in oilseeds. The relatively high initial incorporation of free oleic acid into the *sn*-2 position of PC by in vivo feeding to safflower and sunflower (*Helianthus annuus*) seeds was consistent with this acyl editing mechanism (Griffiths et al., 1988b). In this study, acyl editing is demonstrated as a major in vivo flux for endogenously synthesized FAs. Our previous identification of acyl editing in pea leaves (Bates et al., 2007) and now in developing soybeans suggests that PC acyl editing may be a ubiquitous part of plant lipid metabolism. TAG synthesis in the cell must accommodate acyl editing; indeed, TAG composition may be significantly influenced by its action. However, there are likely to be more fundamental reasons for acyl editing mechanisms. First, it may be important in membrane dynamics and homeostasis. Control of the low level of lyso-PC may be critically important due to its detergent effects on membranes. Second, during periods of high FA synthesis, acyl editing ensures that levels of saturated-oleoyl and dioleoyl molecular species of membrane phospholipids (which may affect membrane fluidity, especially in the cold; Wallis and Browse, 2002) are kept low. Third, a high cycling rate allows for rapid metabolic changes in times of stress. Thus, there is an advantage of adaptability for membrane biogenesis. In addition, cycles in biology add robustness to metabolic networks. Fourth, PC appears to be the acyl flux bank of the plant cell, rather than other phospholipids, such as PE or PI (Browse and Somerville, 1991). The idea that a PC:lyso-PC cycle is the principle acyl acceptor system in the cytosol of the plant cell is reinforced by the metabolic analysis we performed on the *fatB* mutant, where additional acyl flux was directed into PC and PC acyl cycling increased (Bonaventure et al., 2004). Finally, acyl editing may allow for the removal of oxidized acyl groups in membrane lipids.

In seed, as in leaf, PC acyl editing is an order of magnitude greater than PE editing. Also, seed acyl editing of PC at the *sn*-2 position appears dominant over that at the *sn*-1 position. This coincides with in vitro measurements of LPCAT with endogenous lyso-PC acceptor in microsomes from developing soybeans, where >90% of the measured activity is at the *sn*-2 position (Demandre et al., 1994). A high level of *sn*-2 acyl editing is also observed by labeling with nascent FAs or exogenous oleate. However, it is important to note that there is a much greater cyclic flux of acyl editing that is inferred but that cannot be directly measured, so that the real ratio of *sn*-1 to *sn*-2 acyl editing could be significantly higher than 14:86. In this context, sunflower seed microsomes showed similar acyltransferase activity when challenged with *sn*-1 or *sn*-2 ether analogs of lyso-PC, similar to activity with 1-acyl-lyso-PC (Sperling and Heinz, 1993), so we expect that any 2-acyl-lyso-PC produced in vivo will be readily acylated. Additional in vitro studies with 2-acyl-lyso-PC also suggest this outcome (Rochester and Bishop, 1984; Demandre et al., 1994). Exogenous palmitic acid fed to sliced safflower and sunflower cotyledons was directly incorporated into the *sn*-1 position of PC (Griffiths et al., 1988b). Assays of lyso-PL acyltransferase activity in microsomes from developing soybean cotyledons with exogenous acceptor show a higher V_{max} for LPEAT than LPCAT, but with endogenous lyso-lipid acceptors the LPCAT activity was significantly higher (Rajasekharan and Nachiappan, 1994). Further experiments are required to reveal whether lyso-PC generation is by way of a phospholipase A and/or a transacylase (e.g. acyl exchange by a reversal of LPCAT) mechanism.

DAG-PC Interconversion and Localization of DAG Pools

In leaf tissue, DAG is a very minor glycerolipid. From this observation alone it may be inferred that CPT operates in the direction DAG → PC, with a relatively slow reverse reaction. As DAG is a component of lipid signaling cascades (Wang, 2004), cellular control of DAG is likely to be tight. Thus, our finding that there are at least two and probably three kinetically distinct DAG pools is hardly surprising. CPT would certainly be associated with the de novo DAG synthesis pool. Whether the reverse CPT reaction would also produce the DAG pool required for TAG synthesis is debatable. For CPT to provide a flux running in the reverse direction from that associated with de novo glycerolipid synthesis would require a CPT with a locally different equilibrium position, possibly provided by association with a CMP-binding protein (as opposed to an association with the cholinephosphate cytidyltransferase at the input site) and/or a DAG removal mechanism, such as phase partitioning to another membrane domain. It is also possible that a phospholipase C like activity generates much of the bulk DAG pool for TAG synthesis from bulk PC. Thus, there may be no absolute requirement

for a rapidly reversible DAG-PC interconversion. However, differential labeling of PC molecular species with glycerol and phosphocholine dual labeling experiments using linseed required a bulk PC-to-DAG conversion that is independent of de novo DAG synthesis (Slack et al., 1983). The lack of a phospholipase C activity but the presence of a reverse CPT activity in linseed microsomes led these authors to propose that the bulk PC-to-DAG conversion in vivo was via the latter reaction (Slack et al., 1983, 1985).

The identification of distinct kinetic DAG pools raises the question of localization. In a comparative study of CPT and DGAT in microsomes from several different seeds (Vogel and Browse, 1996), the authors concluded that the exclusion of unusual FAs from membrane lipids was not achieved on the basis of CPT or DGAT specificities and postulated distinctly separate pools of DAG as an explanation. The concept of different endomembrane domains is well known (Staehelin, 1997). However, the location of the de novo DAG pool is unclear. Our kinetic analysis suggests that DAG input and output pools may feed to and from a discrete PC pool(s) rather than the bulk PC pool. This discrete PC pool may itself have a more complex structure than we show, with each DAG pool representing separate ER subdomain or connectivity. However, the major portion of total cellular DAG is certainly associated with the oil bodies (Slack et al., 1980). It is a reasonable hypothesis that DAG partitions along with TAG into the oil bodies during their biogenesis as demonstrated in mammalian adipocytes (Kuerschner et al., 2008).

TAG Synthesis

Despite the identification of at least three classes of genes that encode for enzymes of TAG synthesis in plants, and the observation that DGAT1 and DGAT2 proteins from tung seeds, when tagged, localize to different ER domains in tobacco and onion epidermal cells (Shockey et al., 2006), the identification of kinetically distinct routes for TAG synthesis with a preference for saturated or PUFA was unexpected. It raises questions about acyltransferase genes, enzyme specificity, and acyl-CoA channeling.

The synthesis of TAG highly enriched with saturates at the *sn*-3 position presumably requires a DGAT activity, and not PDAT, as it uses nascent FAs directly. Furthermore, PDAT would transfer unsaturates from the *sn*-2 position of PC (Dahlqvist et al., 2000). No specificity information is available for recombinant DGAT and PDAT enzymes from soybean, so comparisons must be made with other plant species. It is unclear whether DGAT1 might provide enriched saturates at the *sn*-3 position. The *dgat1* mutant of Arabidopsis (*Arabidopsis thaliana*) has a slight increase in total saturates in TAG, with the fraction in the *sn*-3 position decreasing only slightly (Katavic et al., 1995), implying little preference for saturates. However, the level of eicosenoic acid at the *sn*-3 position drops dramatically. DGAT2 has been implicated in the production of TAG containing either high amounts of conjugated unsaturated FAs (Shockey et al., 2006) or of ricinoleic acid (Kroon et al., 2006) and on this basis also does not seem to be a good candidate for specific incorporation of saturated acyl groups into TAG. Both recombinant tung DGAT1 and DGAT2 have been assayed in vitro and show little specificity distinction between 16:0, 18:1, 18:2, and 18:3 acyl-CoA substrates (Shockey et al., 2006). Perhaps another DGAT is responsible? The DGAT involved would have a very strong selectivity for saturates if it uses the mixed acyl-CoA pool. However, an alternative scenario concerns possible acyl group channeling via acyl-CoA binding proteins. Numerous such proteins are found in plants (Engeseth et al., 1996; Li and Chye, 2003; Leung et al., 2004; Burton et al., 2005; Kojima et al., 2007), and they may be involved in shuttling acyl groups to different fates. Selective transfer of newly synthesized saturated acyl groups to DGAT via a specific ACBP may have produced the observed kinetics.

Considering the synthesis of TAG that is highly enriched with PUFA at the *sn*-3 position, including tri-PUFA TAG species, both DGAT and PDAT mechanisms may be invoked. Both are shown in Figure 10. TAG synthesis via various transacylases of the PDAT family would transfer a *sn*-2 PUFA from PC to *sn*-3 DAG, producing TAG and lyso-PC (Dahlqvist et al., 2000; Stahl et al., 2004). Thus, PDAT would leave a footprint indistinguishable from *sn*-2 acyl editing. However, it cannot be the major producer of lyso-PC for acyl editing because it would not allow recycling of FA to feed de novo glycerolipid synthesis. For a putative DGAT to be involved, it would either have to have a strong preference for PUFA acyl-CoAs or such molecules would have to be preferentially delivered to the site of the enzyme(s). It is noteworthy that highly *sn*-2-labeled PC from acyl editing is not immediately available for conversion to DAG and then to TAG; otherwise, TAG would contain more *sn*-2 label at early time points. A simple explanation for this is that the bulk PC pool that fills from acyl editing creates a kinetic delay in its use.

CONCLUSION

Through in vivo labeling experiments, we have shown that an acyl editing cycle and kinetically distinct pools of DAG are required to describe the synthesis of TAG in developing soybeans. Similar research in pea seedlings suggests that acyl editing may be a ubiquitous and major flux of plant acyl lipid metabolism (Bates et al., 2007). Many of the individual enzymes/genes that are involved in these processes are unknown or uncertain. As there are many genes in Arabidopsis annotated as acyl transferases or lipases but of unspecified function (Beisson et al., 2003), further research on the acyl editing mechanism to determine if lipases or transacylases are involved is

required. It is possible that not all the gene products/routes in the acylglycerol metabolism (Fig. 10) have been identified. The use of quantitative acyl flux analysis taking into account acyl editing with mutant lines and with targeted knockouts may provide further clues to new genes with overlapping roles in the processes.

Soybean oil is a major worldwide source of vegetable oil, with genetically engineered oil compositions in commercial production and under development. Our quantification of the major flux reactions of acyl groups from synthesis in the plastid to accumulation in TAG may allow a more directed approach toward identifying enzymes that might be useful in oilseed engineering. The enzymatic reactions involved in acyl editing may also be important for transferring unusual FA from their site of synthesis on *sn*-2 PC to the three backbone locations of TAG. The synthesis of TAG and phospholipids must be intricately coordinated because both products require the synthesis of DAG. Production of different lipids from DAG may be controlled by using multiple DAG pools in different locations. Identification of the sites and enzymes in each location may allow more efficient engineering of novel lipid metabolizing enzymes to their site of action in oilseed crop plants. Thus, a better understanding of the pathways of TAG biosynthesis, including acyl editing and DAG production in developing soybeans, may aid future efforts to engineer soybeans with increased oil or with novel compositions.

MATERIALS AND METHODS

Plant Material

Immature pods were harvested from soybean plants (*Glycine max* 'Amsoy') grown in the greenhouse at 24°C to 27°C, supplemented with lights to maintain a 15-h day. Seeds at the R5-R5.5 stage (Egli, 2004) were removed and surface sterilized. After dissection, the embryos were cultured in media containing the carbohydrates, amino acids, inorganic salts, and light conditions required for embryo growth to mimic in planta development as described previously (Allen et al., 2007, 2009). This medium included Suc (140 mM), Glc (70 mM), Gln (35 mM), and Asn (12.6 mM), plus inorganic nutrients (modified Linsamaier-Skoog medium) and Gamborg's vitamins. Harvested embryos (approximately 21 mg dry weight/embryo for [^{14}C]acetate labeling and approximately 15 mg dry weight/embryo for [^{14}C]glycerol labeling) were equilibrated in culture media for 3 d under continuous green light at 30 to 40 μmol m^{-2} s^{-1} before starting labeling experiments.

[^{14}C]Acetate and [^{14}C]Glycerol Labeling

[1-^{14}C]Acetic acid, sodium salt (specific activity 50 mCi/mmol), and [^{14}C(U)]glycerol (specific activity 150 mCi/mmol) were from American Radiolabeled Chemicals. Precultured embryos were transferred to a single beaker containing fresh culture media plus [^{14}C]acetate (1 mM) or [^{14}C]glycerol (0.5 mM) substrate to start the labeling reaction. The media volume was just enough to cover all the embryos and was gently shaken in a water bath at 27°C under 30 to 40 μmol m^{-2} s^{-1} of white light. At each time point, the labeling reaction was quenched by transferring three embryos (four during [^{14}C]glycerol labeling) to 6 mL of 85°C isopropanol for 10 min. The quenching reaction is essential to inactivate phospholipases because, if ignored, large amounts of phospholipid artifacts are generated (Roughan et al., 1978; Slack et al., 1978). In vivo labeling with excised plant tissue can produce considerable variance between samples due to differences in development and in uptake of substrate. To minimize such variance, each data point for total incorporation into lipids was normalized against the trend line for all time points to allow improved kinetic plots (Figs. 2 and 7A).

General Methods

The quenched tissue was homogenized using a mortar and pestle and lipids were extracted with hexane/isopropanol (Hara and Radin, 1978). Radioactivity in the total lipid samples, eluted lipids, or organic and aqueous phases recovered from transmethylation was quantified by liquid scintillation counting. Radioactivity on TLC plates was visualized and quantified by electronic radiography (Instant Imager; Packard Instrument). Silver nitrate-TLC ($AgNO_3$-TLC) plates were prepared by impregnating Partisil K6 silica gel 60 Å TLC plates (Whatman) with 10% $AgNO_3$ in acetonitrile (w/v), drying in air, and activating at 110°C for 5 min. Unlabeled FAMEs were quantified by gas chromatography using a flame ionization detection and a DB-23 capillary column (30 m length × 0.25 mm i.d., 0.25 μ film thickness; J&W). For preparative TLC, all solvents contained 0.01% (w/v) butylated hydroxytoluene antioxidant.

Lipid Class Analysis

Methods for polar lipid separation by TLC, recovery of polar lipids from TLC plates, PC molecular species separation, and positional analysis of PC acyl groups using phospholipase A2 were accomplished as reported previously (Bates et al., 2007). For DAG and TAG analysis, an aliquot of the total lipids was acetylated by standing overnight in acetic anhydride/pyridine (3:2, v/v) and then separating the 1,2-diacyl-3-acetylglycerols (acetylated DAG) from TAG by silica TLC developed in hexane/diethyl ether/acetic acid (70:30:1, v/v/v). Individual neutral lipids were eluted from TLC silica with chloroform/methanol (4:1, v/v). Methanol and 0.88% aqueous KCl were added to give chloroform/methanol/water ratios of 2:1:1 (v/v/v), resulting in a phase separation. The aqueous phase was back extracted with chloroform and lipids were recovered from the combined chloroform extracts.

Analysis of Radiolabeled Acyl Groups

FAMEs were prepared from total lipid extracts by heating to 80°C in 5% H_2SO_4 in methanol (v/v) for 60 min. On cooling and the addition of water, the FAMEs were extracted into hexane. FAMEs were prepared from TLC-purified lipids by base-catalyzed transmethylation (Ichihara et al., 1996). For [^{14}C]glycerol-labeled lipids, the proportion of label in the acyl groups versus the backbone/head-group was determined by transmethylation (Ichihara et al., 1996) and scintillation counting of the separated organic and aqueous phases. Aqueous phase radioactivity from PC was determined to be in the glycerol backbone and not the choline moiety, as reported previously (Bates et al., 2007). [^{14}C]FAME compositions were determined by separation based on the number of double bonds by $AgNO_3$-TLC, the plates being developed to three-quarters height with hexane/diethyl ether (1:1, v/v), and then fully with hexane/diethyl ether (9:1, v/v). Saturated FAMEs were further analyzed by elution from $AgNO_3$-TLC bands with $CHCl_3$/MeOH (2:1, v/v) and separated on KC18 reversed phase silica gel 60 Å TLC plates (Whatman) by development in acetonitrile/methanol/water (65/35/0.5, v/v/v).

Molecular Species Separation of Radiolabeled DAG and TAG

Acetylated DAG was fractionated into molecular species based on the number of double bonds by $AgNO_3$-TLC (Christie, 2003) using a triple development (one-half then three-quarters development in chloroform/methanol [96:4, v/v] and then fully in chloroform/methanol [99:1, v/v]). When necessary, the partially overlapping SD and MM molecular species were eluted from the silica (Christie, 2003) together and further separated on 15% $AgNO_3$-TLC plates at −20°C with the same triple development as above. TAG molecular species fractionation required two distinct $AgNO_3$-TLC separations, both at −20°C. The more saturated species (zero to four double bonds) were separated by triple development (first 60% then 75% development in chloroform/methanol [96:4, v/v] and then fully in chloroform/methanol [98:2, v/v]). The more unsaturated species (five to nine double bonds) were separated by triple development (60%, 75%, and then full development in chloroform/methanol [94:6, v/v]). When necessary, the overlapping SMM

and SSD TAG molecular species were eluted together and separated by $AgNO_3$ TLC at −20°C by triple development in chloroform/methanol (99:1, v/v). The proportion of radioactivity in each molecular species band for DAG and TAG was determined and then each band was eluted, the recovered lipids transmethylated, and the [^{14}C]FAME analyzed by $AgNO_3$-TLC as described above.

Regiochemistry of Radiolabeled DAG and TAG

Purified acetylated DAG and TAG were digested with porcine pancreatic lipase (Christie, 2003). The digestion products were separated on silica TLC developed with hexane/diethyl ether/acetic acid (70:30:2, v/v/v). The amount of radioactivity in MAG, DAG, free FAs, and residual TAG was quantified and then each band was eluted, the recovered lipids transmethylated, and the [^{14}C]FAME analyzed by $AgNO_3$-TLC as described above.

Endogenous Molecular Species Compositions

Total lipids from four soybean embryos (13–14 mg dry weight), cultured under identical conditions to those used for labeling, were extracted according to Hara and Radin (1978). TAG concentrations were measured by direct infusion using electrospray ionization mass spectrometry (ESI-MS; Han and Gross, 2001). ESI-MS was performed in positive ion mode on ammonium adducts. DAG and PC isolated by preparative TLC were converted to their 1,2-diacyl-3-acetyl-*sn*-glycerol (ac-TAG) derivatives by digestion with pancreatic lipase C (for PC) followed by acetylation prior to ESI-MS analysis. Details of instrument operating parameters and quantification are provided online. When necessary, ESI-MS/MS was used to determine the relative abundance of isomers with the same mass-to-charge ratio value. The moles embryo^{-1} of each molecular species measured for TAG, DAG, and PC are provided in Supplemental Tables S1 and S2. All data are reported with SDS for four determinations.

Supplemental Data

The following materials are available in the online version of this article.

Supplemental Figure S1. [^{14}C]Fatty acid composition of total [^{14}C]acetate labeled soybean lipids.

Supplemental Figure S2. α-Oxidation of [^{14}C]acetate labeled saturated FA from TAG and PC.

Supplemental Figure S3. [^{14}C]Acetate-labeled PC molecular species time course.

Supplemental Figure S4. [^{14}C]Acetate-labeled DAG molecular species time course.

Supplemental Figure S5. [^{14}C]Acetate-labeled TAG molecular species time course.

Supplemental Figure S6. [^{14}C]Glycerol-labeled molecular species time course of PC and DAG.

Supplemental Figure S7. Fatty acid composition of [^{14}C]glycerol-labeled TAG, DAG, and PC molecular species.

Supplemental Figure S8. Flux models for TAG synthesis, which were tested by pool filling simulations of kinetic labeling experiments.

Supplemental Figure S9. Pool filling simulations of models shown in Supplemental Figure S8 to describe the kinetic labeling experiments.

Supplemental Table S1. TAG molecular species composition in developing soybean embryos.

Supplemental Table S2. DAG and PC molecular species composition in developing soybean embryos.

Supplemental Table S3. TAG synthesis modeling: nascent FA flux value calculations.

Supplemental Discussion S1. Interconversion of DAG and PC and the supply of DAG for TAG synthesis.

Supplemental Discussion S2. A flux model for glycerolipid synthesis in developing soybean embryos.

Supplemental Methods for Supplemental Figure S2. Chemical α-oxidation.

Supplemental Methods for Supplemental Tables S1 and S2. Endogenous molecular species compositions.

ACKNOWLEDGMENTS

We thank Dr. Doug Allen (Department of Plant Biology, Michigan State University) for assisting us in setting up the soybean embryo culture and the Mass Spectrometry Facility at Michigan State University for ESI-MS.

Received February 24, 2009; accepted March 24, 2009; published March 27, 2009.

LITERATURE CITED

Allen DK, Ohlrogge JB, Shachar-Hill Y (2009) The role of light in soybean seed filling metabolism. Plant J **58:** 220–234

Allen DK, Shachar-Hill Y, Ohlrogge JB (2007) Compartment-specific labeling information in C-13 metabolic flux analysis of plants. Phytochemistry **68:** 2197–2210

Andrews J, Keegstra K (1983) Acyl-CoA synthetase is located in the outer-membrane and acyl-CoA thioesterase in the inner membrane of pea chloroplast envelopes. Plant Physiol **72:** 735–740

Bafor M, Smith MA, Jonsson L, Stobart K, Stymne S (1991) Ricinoleic acid biosynthesis and triacylglycerol assembly in microsomal preparations from developing castor-bean (*Ricinus communis*) endosperm. Biochem J **280:** 507–514

Bates PD, Ohlrogge JB, Pollard M (2007) Incorporation of newly synthesized fatty acids into cytosolic glycerolipids in pea leaves occurs via acyl editing. J Biol Chem **282:** 31206–31216

Beisson F, Koo AJK, Ruuska S, Schwender J, Pollard M, Thelen JJ, Paddock T, Salas JJ, Savage L, Milcamps A, et al (2003) Arabidopsis genes involved in acyl lipid metabolism. A 2003 census of the candidates, a study of the distribution of expressed sequence tags in organs, and a Web-based database. Plant Physiol **132:** 681–697

Block MA, Dorne AJ, Joyard J, Douce R (1983) The acyl-CoA synthetase and acyl-coA thioesterase are located on the outer and inner membrane of the chloroplast envelope, respectively. FEBS Lett **153:** 377–381

Bonaventure G, Ba XM, Ohlrogge J, Pollard M (2004) Metabolic responses to the reduction in palmitate caused by disruption of the FATB gene in Arabidopsis. Plant Physiol **135:** 1269–1279

Brockerhoff H, Yurkowski M (1966) Stereospecific analyses of several vegetable fats. J Lipid Res **7:** 62–64

Browse J, Somerville C (1991) Glycerolipid synthesis: biochemistry and regulation. Annu Rev Plant Physiol Plant Mol Biol **42:** 467–506

Burton M, Rose TM, Faergeman NJ, Knudsen J (2005) Evolution of the acyl-CoA binding protein (ACBP). Biochem J **392:** 299–307

Christie WW (2003) Lipid Analysis: Isolation, Separation, Identification and Structural Analysis of Lipids, Ed 3. The Oily Press, an imprint of PJ Barnes & Associates, Bridgwater, UK

Dahlqvist A, Stahl U, Lenman M, Banas A, Lee M, Sandager L, Ronne H, Stymne H (2000) Phospholipid:diacylglycerol acyltransferase: an enzyme that catalyzes the acyl-CoA-independent formation of triacylglycerol in yeast and plants. Proc Natl Acad Sci USA **97:** 6487–6492

Demandre C, Bahl J, Serghini H, Alpha MJ, Mazliak P (1994) Phosphatidylcholine molecular-species formed by lysophosphatidylcholine acyltransferase from soybean microsomes. Phytochemistry **35:** 1171–1175

Egli DB (2004) Seed-fill duration and yield of crop grains. Adv Agron **83:** 243–271

Engeseth NJ, Pacovsky RS, Newman T, Ohlrogge JB (1996) Characterization of an acyl-CoA-binding protein from *Arabidopsis thaliana*. Arch Biochem Biophys **331:** 55–62

Griffiths G, Stymne S, Stobart AK (1988a) Phosphatidylcholine and its relationship to triacylglycerol biosynthesis in oil-tissues. Phytochemistry **27:** 2089–2093

Griffiths G, Stymne S, Stobart AK (1988b) The utilization of fatty-acid substrates in triacylglycerol biosynthesis by tissue slices of developing safflower (*Carthamus tinctorius* L) and sunflower (*Helianthus annuus* L) cotyledons. Planta **173:** 309–316

Han XL, Gross RW (2001) Quantitative analysis and molecular species

fingerprinting of triacylglyceride molecular species directly from lipid extracts of biological samples by electrospray ionization tandem mass spectrometry. Anal Biochem **295:** 88–100

Hara A, Radin NS (1978) Lipid extraction of tissues with a low-toxicity solvent. Anal Biochem **90:** 420–426

Harwood JL (1996) Recent advances in the biosynthesis of plant fatty acids. Biochim Biophys Acta **1301:** 7–56

Hobbs DH, Lu CF, Hills MJ (1999) Cloning of a cDNA encoding diacylglycerol acyltransferase from *Arabidopsis thaliana* and its functional expression. FEBS Lett **452:** 145–149

Ichihara K, Mae K, Sano Y, Tanaka K (1995) 1-Acylglycerophosphocholine O-acyltransferase in maturing safflower seeds. Planta **196:** 551–557

Ichihara K, Shibahara A, Yamamoto K, Nakayama T (1996) An improved method for rapid analysis of the fatty acids of glycerolipids. Lipids **31:** 535–539

Katavic V, Reed DW, Taylor DC, Giblin EM, Barton DL, Zou JT, Mackenzie SL, Covello PS, Kunst L (1995) Alteration of seed fatty-acid composition by an ethyl methanesulfonate-induced mutation in *Arabidopsis thaliana* affecting diacylglycerol acyltransferase activity. Plant Physiol **108:** 399–409

Kojima M, Casteel J, Miernyk JA, Thelen JJ (2007) The effects of down-regulating expression of *Arabidopsis thaliana* membrane-associated acyl-CoA binding protein 2 on acyl-lipid composition. Plant Sci **172:** 36–44

Koo AJK, Ohlrogge JB, Pollard M (2004) On the export of fatty acids from the chloroplast. J Biol Chem **279:** 16101–16110

Kroon JTM, Wei W, Simon WJ, Slabas AR (2006) Identification and functional expression of a type 2 acyl-CoA:diacylglycerol acyltransferase (DGAT2) in developing castor bean seeds which has high homology to the major triglyceride biosynthetic enzyme of fungi and animals. Phytochemistry **67:** 2541–2549

Kuerschner L, Moessinger C, Thiele C (2008) Imaging of lipid biosynthesis: how a neutral lipid enters lipid droplets. Traffic **9:** 338–352

Lands WEM (1965) Lipid metabolism. Annu Rev Biochem **34:** 313–346

Lardizabal KD, Mai JT, Wagner NW, Wyrick A, Voelker T, Hawkins DJ (2001) DGAT2 is a new diacylglycerol acyltransferase gene family: purification, cloning, and expression in insect cells of two polypeptides from *Mortierella ramanniana* with diacylglycerol acyltransferase activity. J Biol Chem **276:** 38862–38869

Leung KC, Li HY, Mishra G, Chye ML (2004) ACBP4 and ACBP5, novel Arabidopsis acyl-CoA-binding proteins with kelch motifs that bind oleoyl-CoA. Plant Mol Biol **55:** 297–309

Li HY, Chye ML (2003) Membrane localization of Arabidopsis acyl-CoA binding protein ACBP2. Plant Mol Biol **51:** 483–492

Napier JA (2007) The production of unusual fatty acids in transgenic plants. Annu Rev Plant Biol **58:** 295–319

Ohlrogge J, Browse J (1995) Lipid biosynthesis. Plant Cell **7:** 957–970

Ohlrogge JB, Kuhn DN, Stumpf PK (1979) Subcellular-localization of acyl carrier protein in leaf protoplasts of *Spinacia oleracea*. Proc Natl Acad Sci USA **76:** 1194–1198

Pollard M, Ohlrogge J (1999) Testing models of fatty acid transfer and lipid synthesis in spinach leaf using in vivo oxygen-18 labeling. Plant Physiol **121:** 1217–1226

Rajasekharan R, Nachiappan V (1994) Use of photoreactive substrates for characterization of lysophosphatidate acyltransferases from developing soybean cotyledons. Arch Biochem Biophys **311:** 389–394

Rochester CP, Bishop DG (1984) The role of lysophosphatidylcholine in lipid-synthesis by developing sunflower (*Helianthus annuus* L) seed microsomes. Arch Biochem Biophys **232:** 249–258

Roehm JN, Privett OS (1970) Changes in the structure of soybean triglycerides during maturation. Lipids **5:** 353–358

Roughan PG, Slack CR (1982) Cellular organization of glycerolipid metabolism. Annu Rev Plant Physiol Plant Mol Biol **33:** 97–132

Roughan PG, Slack CR, Holland R (1978) Generation of phospholipid artifacts during extraction of developing soybean seeds with methanolic solvents. Lipids **13:** 497–503

Saha S, Enugutti B, Rajakumari S, Rajasekharan R (2006) Cytosolic triacylglycerol biosynthetic pathway in oilseeds. Molecular cloning and expression of peanut cytosolic diacylglycerol acyltransferase. Plant Physiol **141:** 1533–1543

Schwender J, Shachar-Hill Y, Ohlrogge JB (2006) Mitochondrial metabolism in developing embryos of *Brassica napus*. J Biol Chem **281:** 34040–34047

Shindou H, Shimizu T (2009) Acyl-CoA:lysophospholipid acyltransferases. J Biol Chem **284:** 1–5

Shockey JM, Gidda SK, Chapital DC, Kuan JC, Dhanoa PK, Bland JM, Rothstein SJ, Mullen RT, Dyer JM (2006) Tung tree DGAT1 and DGAT2 have nonredundant functions in triacylglycerol biosynthesis and are localized to different subdomains of the endoplasmic reticulum. Plant Cell **18:** 2294–2313

Slack CR, Bertaud WS, Shaw BD, Holland R, Browse J, Wright H (1980) Some studies on the composition and surface properties of oil bodies from the seed cotyledons of safflower (*Carthamus tinctoris*) and linseed (*Limum ustatissimum*). Biochem J **190:** 551–561

Slack CR, Campbell LC, Browse JA, Roughan PG (1983) Some evidence for the reversibility of the cholinephosphotransferase-catalyzed reaction in developing linseed cotyledons in vivo. Biochim Biophys Acta **754:** 10–20

Slack CR, Roughan PG, Balasingham N (1977) Labeling studies in vivo on metabolism of acyl and glycerol moieties of glycerolipids in developing maize leaf. Biochem J **162:** 289–296

Slack CR, Roughan PG, Balasingham N (1978) Labeling of glycerolipids in cotyledons of developing oilseeds by [1-C-14]acetate and [2-H-3]glycerol. Biochem J **170:** 421–433

Slack CR, Roughan PG, Browse JA, Gardiner SE (1985) Some properties of cholinephosphotransferase from developing safflower cotyledons. Biochim Biophys Acta **833:** 438–448

Sperling P, Heinz E (1993) Isomeric *sn*-1-octadecenyl and *sn*-2-octadecenyl analogues of lysophosphatidylcholine as substrates for acylation and desaturation by plant microsomes. Eur J Biochem **213:** 965–971

Sperling P, Linscheid M, Stocker S, Muhlbach HP, Heinz E (1993) In-vivo desaturation of cis-delta-9-monounsaturated to cis-delta-9,12-diunsaturated alkenylether glycerolipids. J Biol Chem **268:** 26935–26940

Staehelin LA (1997) The plant ER: a dynamic organelle composed of a large number of discrete functional domains. Plant J **11:** 1151–1165

Stahl U, Carlsson AS, Lenman M, Dahlqvist A, Huang BQ, Banas W, Banas A, Stymne S (2004) Cloning and functional characterization of a phospholipid:diacylglycerol acyltransferase from Arabidopsis. Plant Physiol **135:** 1324–1335

Stobart K, Mancha M, Lenman M, Dahlqvist A, Stymne S (1997) Triacylglycerols are synthesised and utilized by transacylation reactions in microsomal preparations of developing safflower (*Carthamus tinctorius* L) seeds. Planta **203:** 58–66

Stymne S, Stobart AK (1987) Triacylglycerol biosynthesis. *In* PK Stumpf, ed, The Biochemistry of Plants: A Comprehensive Treatise, Vol 9, Lipids: Structure and Function. Academic Press, New York, pp 175–214

Stymne S, Stobart AK (1984) Evidence for the reversibility of the acyl-CoA-lysophosphatidylcholine acyltransferase in microsomal preparations from developing safflower (*Carthamus tinctorius* L) cotyledons and rat liver. Biochem J **223:** 305–314

Triki S, Demandre C, Mazliak P (1999) Biosynthesis of triacylglycerols by developing sunflower seed microsomes. Phytochemistry **52:** 55–62

Vogel G, Browse J (1996) Cholinephosphotransferase and diacylglycerol acyltransferase (substrate specificities at a key branch point in seed lipid metabolism). Plant Physiol **110:** 923–931

Wallis JG, Browse J (2002) Mutants of Arabidopsis reveal many roles for membrane lipids. Prog Lipid Res **41:** 254–278

Wang XM (2004) Lipid signaling. Curr Opin Plant Biol **7:** 329–336

Zou JT, Wei YD, Jako C, Kumar A, Selvaraj G, Taylor DC (1999) The *Arabidopsis thaliana* TAG1 mutant has a mutation in a diacylglycerol acyltransferase gene. Plant J **19:** 645–653